Cancer Biol Med 2026. doi: 10.20892/j.issn.2095-3941.2025.0261

ORIGINAL ARTICLE

Coordinated DNA methyltransferase 3A and methyltransferase-like 7A activity reprograms the tumor microenvironment through discoidin domain receptor 1 signaling

Zhengyang Bai[1]*, Dan Yang[1]*, Jiayi Li[2]*, Yaobang Liu[3], Bin Lian[3], Jinping Li[3]

[1]The First Clinical Medical School of Ningxia Medical University (General Hospital of Ningxia Medical University), Yinchuan 750004, China; [2]Ningxia Medical University, Yinchuan 750004, China; [3]Department of Surgical Oncology, General Hospital of Ningxia Medical University, Yinchuan 750004, China

ABSTRACT

Objective: Breast cancer is the most common malignancy in women and is characterized by a high recurrence rate that severely impacts patient survival. Regulatory T cells (Tregs) in the tumor microenvironment (TME) promote immune evasion and metastasis, increasing recurrence risk. This study determined how the epigenetic regulators, DNMT3A and METTL7A, modulate Treg infiltration *via* the *DDR1/STAT3/CXCL5* axis and influence breast cancer recurrence and prognosis.

Methods: RNA sequencing (RNA-seq) was used to identify differentially expressed genes (DEGs), followed by Gene Ontology (GO) and Kyoto Encyclopedia of Genes and Genomes (KEGG) enrichment. Machine learning algorithms, including least absolute shrinkage and selection operator (LASSO), supported vector machine-recursive feature elimination (SVM-RFE) and ElasticNet identified DDR1 as a key gene. Validation included RT-qPCR, western blot, MSP, MeRIP-qPCR, and Co-IP to assess epigenetic regulation. Functional assays (CCK-8, Transwell, and Treg differentiation/chemotaxis) and xenograft models evaluated the role of *DDR1* in tumor progression and recurrence.

Results: DNMT3A upregulated *DDR1 via* DNA methylation, while METTL7A enhanced *DDR1* mRNA stability *via* m6A modification. Co-regulation activated the *DDR1/STAT3/CXCL5* axis, which boosted cancer cell proliferation, migration, and invasion. CXCL5 secretion increased Treg infiltration and accelerated tumor growth *in vivo*. *DDR1* silencing reversed these effects, confirming that *DDR1* has a pivotal role in breast cancer recurrence.

Conclusion: DNMT3A and METTL7A were shown to cooperatively regulate *DDR1 via* DNA/m6A methylation, which drives Treg-mediated immune suppression and recurrence. This study provided novel insights and therapeutic targets for breast cancer prognosis and treatment.

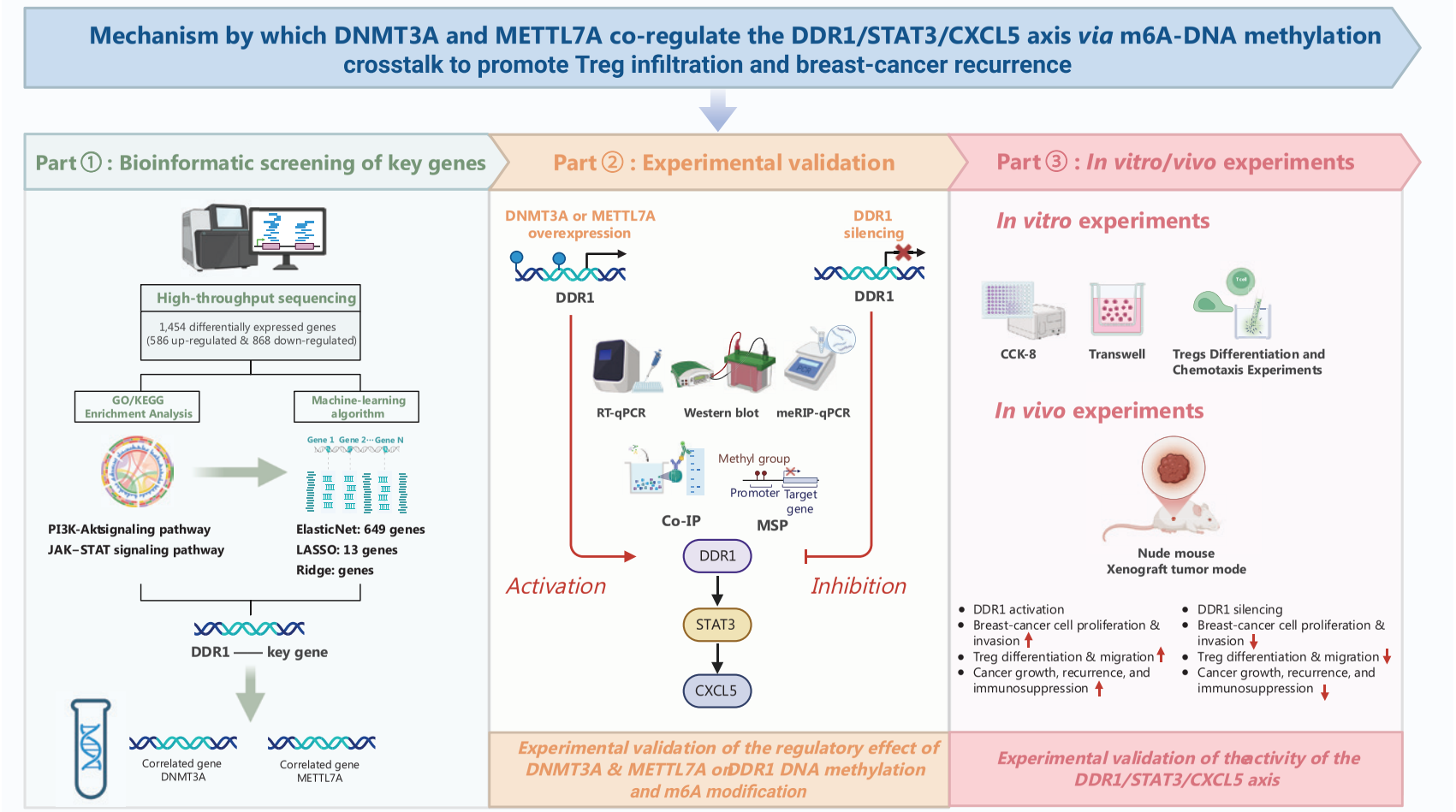
KEYWORDS Tumor microenvironment; DNMT3A; METTL7A; *DDR1/STAT3/CXCL5* axis; Discoidin domain receptor 1

Introduction

Breast cancer, the most prevalent malignancy among women worldwide, poses a significant threat to patient survival due to high recurrence and metastasis rates[1]. Despite advances in diagnosis and treatment, the 5-year survival rate for advanced-stage patients remains suboptimal[2]. The tumor microenvironment (TME) has a pivotal role in breast cancer progression with the immunosuppressive nature representing a major barrier to therapeutic success[3,4]. Regulatory T cells (Tregs), as key components of this immunosuppressive TME, use multiple mechanisms to inhibit anti-tumor immune responses[5-7]. Current Treg-targeted strategies, including Treg depletion and immunosuppressive function blockade, are often limited by insufficient specificity and considerable toxicity[8,9]. Therefore, elucidating the precise regulatory mechanisms underlying Treg infiltration in breast cancer represents an essential research direction in tumor immunology by deepening our understanding of immune evasion and identifying novel targets for precision immunotherapy.

Epigenetic regulation serves as a crucial link between genotype and phenotype with fundamental roles in tumorigenesis

*These authors are regarded as co-first authors.
Correspondence to: Jinping Li
E-mail: 13995105618@163.com
ORCID ID: https://orcid.org/0000-0001-9142-5239
Received May 5, 2025; accepted October 9, 2025.
Available at www.cancerbiomed.org
©2026 The Authors. Creative Commons Attribution-NonCommercial 4.0 International License (CC BY-NC 4.0)



Study flowchart This schematic illustrates the overall design and workflow of the study. Part ①, transcriptome sequencing identified differentially expressed genes (DEGs) between normal mammary epithelial and breast cancer cells, followed by GO/KEGG enrichment analyses and machine-learning algorithms (ElasticNet, LASSO, Ridge, and SVM-RFE), which collectively identified DDR1 as the key gene and revealed its strong correlation with DNMT3A and METTL7A. Part ②, molecular experiments including RT-qPCR, Western blot, MSP, MeRIP-qPCR, and co-immunoprecipitation demonstrated that DNMT3A regulates DDR1 *via* DNA methylation, while METTL7A enhances DDR1 mRNA stability through m6A modification, thereby activating or inhibiting the DDR1/STAT3/CXCL5 signaling axis. Part ③, *in vitro* functional assays (CCK-8, Transwell, and Treg differentiation and chemotaxis assays) and *in vivo* nude mouse xenograft models confirmed that activation of DDR1 promotes breast cancer cell proliferation and invasion, enhances Treg differentiation and infiltration, and accelerates tumor growth and recurrence, whereas DDR1 silencing reverses these effects.

and immune microenvironment remodeling[10-12]. Epigenetic mechanisms shape the immunosuppressive landscape by modulating chemokine secretion and immune checkpoint expression[13,14]. DNA methylation and RNA N^6-methyladenosine (m^6A) modification represent two predominant regulatory layers among various epigenetic modifications that can interact to form cooperative networks[15-17]. Although previous studies have suggested that discoidin domain receptor 1 *(DDR1)* may be involved in tumor-stroma interactions and is regulated by epigenetic mechanisms, the role of *DDR1* in the immune microenvironment, especially with respect to the infiltration of Tregs, has not been established.

DDR1 is an atypical tyrosine kinase receptor within the TME signaling network that functions as a collagen-binding receptor and has a critical role in signal transduction between the extracellular matrix and tumor cells[18,19]. Recent studies have shown that *DDR1* not only participates in the adhesion, migration, and invasion of breast cancer cells but may also mediate immune-related signals to regulate recruitment of immune cells[20]. Specifically, *DDR1* activates the downstream signal transducer and activator of transcription 3 (STAT3) signaling pathway, which subsequently upregulates C-X-C motif chemokine ligand 5 (CXCL5) expression. CXCL5 has a key role in neutrophil and Treg migration[21]. While previous studies have primarily focused on the role of CXCL5 in inflammation and tumor metastasis, the specific mechanism underlying immunosuppressive cell infiltration, such as Tregs, remains elusive[22]. Notably, our previous research demonstrated that *DDR1* is highly expressed in breast cancer tissues and the level of expression is positively correlated with Treg infiltration, suggesting a potential role as a "bridge molecule" linking epigenetic modifications to immune regulation. In addition, CXCL5 has been reported to induce the formation of neutrophil extracellular traps (NETs), further contributing to remodeling of the immune microenvironment and enhancement of immunosuppression[23,24]. Therefore, investigating whether the *DDR1/STAT3/CXCL5* axis has a central role in epigenetically regulated Treg recruitment and tumor immune evasion may provide theoretical support for the identification of novel immunotherapeutic targets.

Advances in high-throughput transcriptome sequencing (RNA-seq) technologies have established multi-omics integration as a powerful approach for elucidating complex biological processes (BPs)[25,26]. Conventional single-omics studies often fail to comprehensively characterize gene regulatory networks, whereas the integration of genomic, transcriptomic, epigenomic, and proteomic data provides a more systematic understanding[27,28]. Machine learning algorithms, such as least absolute shrinkage and selection operator (LASSO) regression and support vector machines (SVMs), have demonstrated remarkable potential in identifying key feature genes from massive datasets and has been shown to be particularly valuable for tumor biomarker discovery and molecular subtyping[29,30]. Critical regulatory nodes were systematically identified in the current study by integrating multi-omics data with machine learning approaches. A DNMT3A-METTL7A-*DDR1* regulatory network was constructed through the combined analysis of methylome, transcriptome, and m^6A epi transcriptome data, along with machine learning methods, including LASSO. This integrated multi-omics strategy offers novel insights into epigenetic-immune regulation.

The current study revealed how DNMT3A and METTL7A cooperatively regulate *DDR1 via* epigenetic coordination, activating the STAT3/CXCL5 axis to promote Treg infiltration. DNMT3A-mediated DNA methylation was shown to regulate *DDR1* transcription, whereas METTL7A-catalyzed m6A modification stabilized *DDR1* mRNA, revealing a previously unrecognized "DNA–RNA dual modification" paradigm. The *DDR1/STAT3/CXCL5* axis was identified as a key regulator of Treg recruitment. Mechanistic insight into the crosstalk between epigenetic regulation and the tumor immune microenvironment (TIME) was provided in the current study by integrating multi-omics analyses with machine learning. Clinically, the *DNMT3A/METTL7A/DDR1* signature has potential as a prognostic biomarker and the *DNMT3A/METTL7A/DDR1* regulatory network may offer novel therapeutic targets for refractory breast cancer, including triple-negative breast cancer (TNBC).

Materials and methods

High-throughput transcriptome sequencing

Sequencing libraries were generated and sequenced by CapitalBio Technology (Beijing, China) using 5 μg of total RNA per sample. Briefly, ribosomal RNA (rRNA) was removed from the total RNA using the Ribo-Zero Magnetic Kit (MRZG12324; Epicentre, Madison, WI, USA). Sequencing libraries were constructed with the NEBNext Ultra RNA Library Prep Kit for Illumina (E7760S; New England Biolabs, Ipswich, MA, USA). RNA was fragmented into ~300 bp fragments in the NEBNext First Strand Synthesis Reaction Buffer (5×). First-strand cDNA was synthesized using reverse transcriptase with random primers, followed by second-strand cDNA synthesis in the presence of dUTP Mix (10×) in the Second Strand Synthesis Reaction Buffer. The cDNA fragments were subjected to end repair, poly(A) tail addition, and Illumina adapter ligation. The USER Enzyme (M5508; NEB) was used to digest the second cDNA strand to construct strand-specific libraries after adapter ligation. Library DNA was amplified, purified, and enriched by PCR. The libraries were qualified using an Agilent 2100 Bioanalyzer (Agilent Technologies, Santa Clara, CA, USA) and quantified with the KAPA Library Quantification Kit (kk3605; Merck, Darmstadt, Germany). RNA-seq experiments were performed in three biological replicates per group on the Illumina NovaSeq platform (Illumina, San Diego, CA, USA) using paired-end 150

bp sequencing and generating an average of 50 million reads per sample[31].

Transcriptome sequencing data analysis

Quality control of raw paired-end sequencing reads was performed using FastQC (v0.11.8). Raw data was processed with Cutadapt (v1.18) to remove Illumina sequencing adapters and poly(A) tail sequences. Reads containing > 5% ambiguous bases (N) were filtered out using a Perl script. The FASTX Toolkit (v0.0.13) was used to retain reads with ≥ 70% of bases that had a Phred quality score > 20. Paired-end reads were error-corrected with BBMap and high-quality reads were aligned to the human reference genome using HISAT2 (v0.7.12).

Differential expression analysis of mRNA read counts was performed using limma ($|\log2FC| > 3$; adj. $P < 0.05$). Gene Ontology (GO) and Kyoto Encyclopedia of Genes and Genomes (KEGG) pathway enrichment analyses were performed with ClusterProfiler and the results were visualized as bubble plots. Feature selection was carried out using glmnet (LASSO, ridge, ElasticNet) and caret (SVM-RFE). Overlapping genes were identified using VennDiagram.

5-methylcytosine (5mC) and m^{6}A gene expression analysis

A literature-curated list of 20 5mC- and 26 m6A-related genes was analyzed. Expression profiles were extracted from transcriptome data and visualized as heatmaps generated with pheatmap (v1.0.12), comparing normal mammary epithelial and breast cancer cells. Pearson correlation analysis (stats package) was used to identify 5mC and m6A genes most strongly associated with *DDR1* expression.

m^{6}A modification site prediction

Potential m^{6}A modification sites on *DDR1* mRNA were predicted using the SRAMP web server. The *DDR1* nucleotide sequence was retrieved from NCBI in FASTA format and submitted to the online tool for analysis.

Cell transduction and experimental groups

Lentiviral particles were produced in HEK293T cells using Lipofectamine 2000 (#11668030; Thermo Fisher, Waltham, MA, USA). pHAGE-puro (#118692; Addgene, Watertown, MA, USA) was co-transfected with pSPAX2 (#12260; Addgene, Watertown, MA, USA) and pMD2.G (#12259; Addgene, Watertown, MA, USA) for overexpression. pSuper-retro-puro was packaged with gag/pol (#14887; Addgene, Watertown, MA, USA) and VSVG (#8454; Addgene, Watertown, MA, USA) for knockdown. Viral supernatants were collected at 48 and 72 h, filtered (0.45 μm), concentrated, pooled, and titrated. Lentiviral transduction of MCF-7 cells was carried out using packaging services provided by Sangon Biotech (Shanghai, China).

MCF-7 cells in logarithmic growth were seeded at 1×10^5 cells/well in 6-well plates. Cells at ~75% confluence were transduced with lentivirus (MOI = 10; ~5×10^6 TU/mL) and 5 μg/mL of polybrene (TR-1003; Merck) for 4 h, followed by medium dilution and replacement after 24 h. Cells were cultured with a stepwise increase in puromycin (2–10 μg/mL, E607054; Sangon Biotech) until no further cell death occurred. Knockdown efficiency was verified by western blot and RT-qPCR (shRNA sequences listed in **Table S1**).

The experimental groups were as follows: control group (MCF-7 cells transduced with empty vector lentivirus); oe-DNMT3A group (MCF-7 cells overexpressing DNMT3A); oe-METTL7A group (MCF-7 cells overexpressing METTL7A); oe-DNMT3A + oe-METTL7A group (MCF-7 cells co-overexpressing DNMT3A and METTL7A); and oe-DNMT3A + oe-METTL7A + sh-*DDR1* group (MCF-7 cells co-overexpressing DNMT3A and METTL7A with *DDR1* knockdown). Each group was tested in triplicate[32].

Site-specific m^{6}A methylated RNA immunoprecipitation (MeRIP)-qPCR assay

The *DDR1* mRNA m^{6}A modification levels were evaluated using the MeRIP m^{6}A kit (17-10499-2; Merck). Co-precipitated samples and input controls were digested with proteinase K and RNA extraction. *DDR1* mRNA enrichment levels were quantified by RT-qPCR with experiments performed in triplicate. The levels of expression were normalized to input controls. The *DDR1* (human) primer sequences were as follows: forward, 5′-GATCTCGACTCCGCTTCAAGGA-3′; and reverse, 5′-CAAAGGGTGTCCCTTACGCACA-3′.

Clonal bisulfite sequencing

DNA methylation analysis at cg13329862 (DDR1) was performed using clonal bisulfite sequencing (CBS). Genomic DNA was extracted with the DNeasy Blood & Tissue Kit (Qiagen, Hilden, Germany) and quantified using a NanoDrop 2000 spectrophotometer (Thermo Fisher). Bisulfite conversion of 500 ng of genomic DNA was performed with the EZ DNA Methylation Kit (Zymo Research, Irvine, CA, USA). Converted DNA was resuspended in 40 μL of TE buffer and stored at −20°C.

PCR amplification was carried out in a 20-μL reaction containing 2 μL of bisulfite-treated DNA, 2 μL of each forward (5′-TGATTTTGGGGTTGTTTGTTAGTA-3′) and reverse (5′-AATACTTTTTCCCCACTCAACACTA-3′) primer (2 μM each), 1× PCR buffer, 10 mM dNTPs (TR1122; Thermo

Fisher), 1 mM $MgCl_2$ (AM9530G; Thermo Fisher), and 1 U ZymoTaq™ DNA polymerase (E2002; Zymo Research). The cycling conditions were as follows: 95°C for 10 min; 35 cycles at 95°C for 30 s, 59°C for 40 s, and 72°C for 1 min; and a final extension at 72°C for 10 min. PCR products were resolved on a 1.5% agarose gel stained with purified GelRed (K310001; Thermo Fisher), and cloned into pCR®4-TOPO® (K4575-02; Thermo Fisher, Waltham, MA, US).

The cloning products were transformed into *E. coli* TOP10 competent cells (Thermo Fisher) and plated on LB/ampicillin (50 μg/mL; Beyotime, China) agar plates. Positive clones were PCR-verified (T3/T7 primers) and sequenced (Genewiz) after an overnight incubation at 37°C. Bisulfite sequencing DNA methylation analysis (BISMA) was used to analyze methylation, excluding redundant clones and sequences with < 95% conversion efficiency. The methylation frequency at target CpGs was calculated statistically.

Co-immunoprecipitation assay

Protein-protein interactions (PPIs) between DDR1 and STAT3 were analyzed using the Pierce Co-immunoprecipitation (Co-IP) Kit (26149; Thermo Fisher). Cell lysates were incubated with DDR1 antibody (ab288675; Abcam, UK)/STAT3 (ab68153; Abcam) or IgG control antibody (ab172730; Abcam), followed by the addition of Protein A/G magnetic beads (ab286842; Abcam) to capture the antigen-antibody complexes. The presence of STAT3 in immunoprecipitates was detected after elution by western blot analysis.

Cell Counting Kit-8 cell viability assay

Cell viability was assessed using the cell counting kit-8 (CCK-8) assay. Cells from each experimental group were seeded in 96-well plates (CLS3922; Corning, USA) at a density of 5×10^3 cells/well ($n = 5$ replicates per group). After 24, 48, and 72 h of culture, 10 μL of CCK-8 reagent (CK04; Dojindo, Japan) was added to each well and incubated at 37°C for 2 h. Absorbance at 450 nm (OD450) was monitored utilizing a microplate reader (168–1130; Bio-Rad, USA) to evaluate cell viability. The experiment was performed in triplicate.

EdU cell proliferation assay

Cells (1×10^5/well) in 24-well plates (Corning) were incubated with 50 μM EdU (RiboBio, Guangzhou, China) for 2 h at 37°C, fixed with 4% paraformaldehyde (Sigma-Aldrich, St. Louis, MO, USA), and stained using Apollo and DAPI (Thermo Fisher). Images were captured using a Leica microscope (Germany) from five randomly selected fields per sample and the number of EdU^+ cells was quantified. All experiments were performed in triplicate.

Colony formation assay

Cells (500/well) were seeded in 6-well plates (TMO140644; Corning) and cultured for 14 d at 37°C with medium replaced every 3 d. The colonies were fixed with 4% paraformaldehyde (158127; Sigma-Aldrich), stained with 0.1% crystal violet (C3886; Sigma-Aldrich), and counted after washing. Experiments were performed in triplicate.

Wound healing assay

Cells were pretreated with 10 μg/mL of mitomycin C (M5353; Sigma-Aldrich) for 2 h. Subsequently, 5×10^5 cells per well were seeded in 6-well plates (3516; Corning) and cultured until > 90% confluence. Uniform wounds were created in the monolayer using a sterile 10-μL pipette tip, followed by 2 gentle washes to remove detached cells. Serum-free medium was added and the wound areas were photographed at 0 and 36 h using an inverted microscope (Olympus, Japan) at identical positions. Wound widths were measured using ImageJ 6.0 software (Media Cybernetics, USA), and cell migration ability was calculated as follows: wound closure (%) = [(width at 0 h – width at 36 h)/width at 0 h] × 100%.

Transwell invasion and migration assays

Cell invasion was assessed using Transwell chambers (8-μm pores; Corning) pre-coated with Matrigel (BD Biosciences), diluted 1:8, and incubated at 37°C for 30 min. After a 12-h serum starvation, 1×10^5 cells/mL in serum-free medium were seeded in upper chambers, while lower chambers contained 600 μL of medium with 10% FBS as a chemoattractant. Following a 24-h incubation, non-invaded cells were removed and the invaded cells were fixed with methanol, stained with 1% crystal violet (Beyotime), then quantified by counting five random fields per membrane. Migration assays were performed using uncoated Transwell chambers (8-μm pore size, 3422; Corning) following the same procedure.

Treg differentiation assay

Human $CD4^+$ T cells (JY-J1251; Shanghai Jinyuan Biotechnology, Shanghai, China) were cultured in RPMI-1640 (11875093; Gibco) supplemented with 10% FBS, 1% penicillin-streptomycin, 10 mM HEPES (15630080; Gibco), 2 mM L-glutamine (G8540; Sigma-Aldrich), 1 mM sodium pyruvate (11360070; Gibco), MEM non-essential amino acids (11140050; Gibco), and 55 μM β-mercaptoethanol (31350010; Gibco). The cells (1×10^6/mL) were stimulated with anti-CD3 (1 μg/mL, 317326; BioLegend) and anti-CD28 (1 μg/mL, 302934; BioLegend) and co-cultured with breast

cancer cells (1:1 ratio) from different treatment groups for 72 h. Flow cytometry (BD LSRFortessa, USA) analyzed CD4+CD25+Foxp3+ Tregs *via* fixation and staining with anti-CD4-FITC (11-0049-42; Invitrogen), anti-CD25-PE (12-0259-42; Invitrogen), and anti-Foxp3-Alexa Fluor 647 (560045; BD Biosciences), per manufacturers' protocols, followed by data analysis using FlowJo (v10.7.1) was accessed as a commercial software[32].

Chemotaxis assay

Treg migration was evaluated using Transwell chambers (8 μm-pore; Corning) with 600 μL of 10% FBS medium (1:1 mixed with conditioned medium) in the lower chamber and 5×10^5 $CD4^+$ T cells (serum-free) in the upper chamber. Non-migrated cells were removed after 12 h, while migrated cells were fixed in 4% PFA for 30 min, stained with 0.1% crystal violet for 20 min, dried, and counted in five random fields.

Animal model establishment and grouping

Female nude mice (BALB/c, 4–6 weeks old; Charles River, China) were maintained under specific pathogen-free (SPF) conditions at 22 ± 2°C with 50 ± 10% humidity and 12 h light/dark cycles. The mice had access to standard chow and sterile water *ad libitum*. Breast cancer xenografts were established by subcutaneously injecting 1×10^6 MCF-7 cells in 100 μL of PBS with different genetic modifications into the right flank under sterile conditions. All animal procedures were approved by the Ethics Committee of the General Hospital of Ningxia Medical University (Approval No.: KYLL-2025-1285) and performed in compliance with ethical guidelines to minimize suffering.

The experimental groups ($n = 6$ per group) were as follows: control (empty vector-transduced MCF-7 cells); oe-DNMT3A (DNMT3A-overexpressing cells); oe-METTL7A (METTL7A-overexpressing cells); oe-DNMT3A + oe-METTL7A (dual-overexpressing cells); and oe-DNMT3A + oe-METTL7A + sh-*DDR1* (dual-overexpressing with *DDR1* knockdown). Tumor growth was measured every 3 d using calipers (Mitutoyo, Japan) and the volume (V) was calculated as 0.5 × length (L) × width $(W)^2$. At day 21 post-inoculation, the tumors were surgically excised, weighed (Mettler Toledo, Switzerland), and recurrence rates and times were monitored for 15 d post-excision[33].

Flow cytometric analysis of tumor-infiltrating Tregs

Single-cell suspensions were prepared from tumor tissues using a Tumor Dissociation Kit (#130-096-730; Miltenyi Biotec). Cells were stained with anti-CD4-FITC (1:200, #100405; BioLegend), anti-CD25-PE (1:100, #113703; BioLegend), and anti-Foxp3-Alexa Fluor 647 (1:100, #126407; BioLegend) for 30 min after RBC lysis (#R7757; Sigma-Aldrich). Intracellular fixation/permeabilization was performed using eBioscience buffers™ (#88-8824-00 and #00-5523-00; Thermo Fisher). Flow cytometry and FlowJo analysis quantified CD4+CD25+Foxp3+ Tregs among tumor-infiltrating lymphocytes.

Statistical analysis

Data are presented as the mean ± SD from ≥ 3 independent experiments. Two-group comparisons were performed using an independent samples *t*-test, multiple-group comparisons were performed using one-way analysis of variance (ANOVA), and data from different time points were analyzed using two-way ANOVA. Analyses were performed in GraphPad GraphPad Prism 9.5.0 (GraphPad Software, San Diego, CA, USA) and R 4.2.1 (R Foundation for Statistical Computing, Vienna, Austria) with $*P* < 0.05$ considered significant.

Results

Bioinformatics reveals that discoidin domain receptor 1 is epigenetically regulated to promote regulatory T cell infiltration in breast cancer

RNA-seq analysis of MCF-10A (normal mammary epithelial) and MCF-7 (breast cancer) cells (**Figure 1A**) identified 1454 DEGs ($|\log2FC| > 3$; adj. $P < 0.05$), including 586 upregulated and 868 downregulated genes (**Figure 1B**). GO analysis revealed enrichment in epidermal development (biological process [BP]), collagen-containing extracellular matrix (cellular component [CC]), and receptor–ligand activity (molecular function [MF]; **Figure 1C**). KEGG analysis indicated enrichment in the PI3K–Akt and JAK–STAT signaling pathways (**Figure 1D**). We next focused on the JAK/STAT3 pathway because recent evidence suggested that *DDR1* not only promotes breast cancer cell adhesion, migration, and invasion but also mediates immune-related signaling that regulates immune cell recruitment[20]. Specifically, *DDR1* activates downstream STAT3 signaling, inducing CXCL5 expression, a chemokine essential for neutrophil and Treg migration[21].

Four machine learning algorithms were used to screen the DEGs to identify key genes involved in the onset and progression of breast cancer, which resulted in the identification of 649 genes using the ElasticNet algorithm (**Figure 1E**), 13 genes using the LASSO algorithm (**Figure 1F**), 9 genes using the Ridge algorithm (**Figure 1G**), and 5 genes using the SVM-RFE algorithm (**Figure 1H**). The intersection of these results yielded a single common gene, *DDR1*,

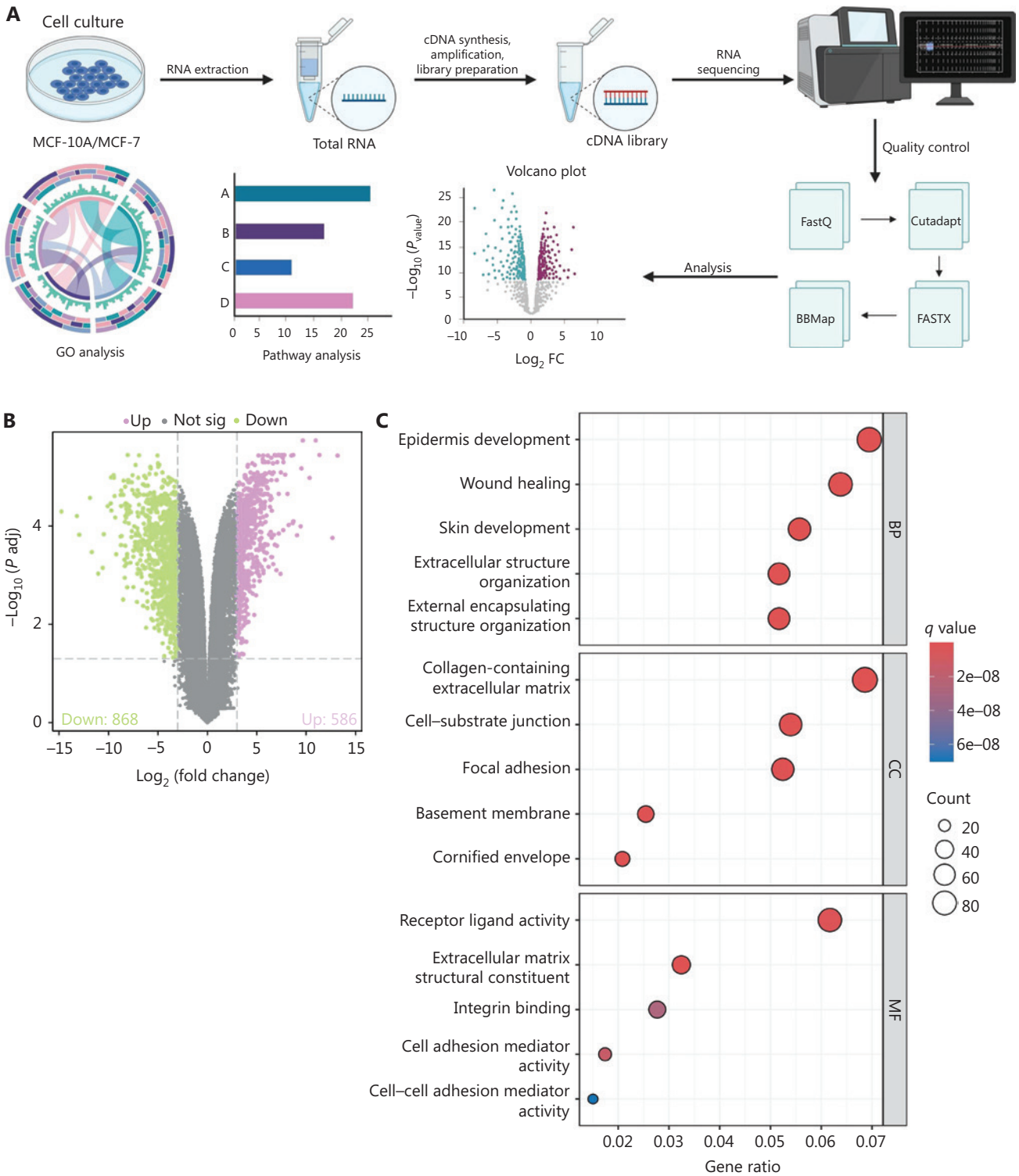


Figure 1 Continued

highlighting its critical role in breast cancer progression. Thus, *DDR1* was selected as the core candidate gene (**Figure 1I**), which was significantly upregulated in breast cancer tissues (**Figure 1J**). These findings suggested that *DDR1* has a crucial role in regulating the development and progression of breast cancer.

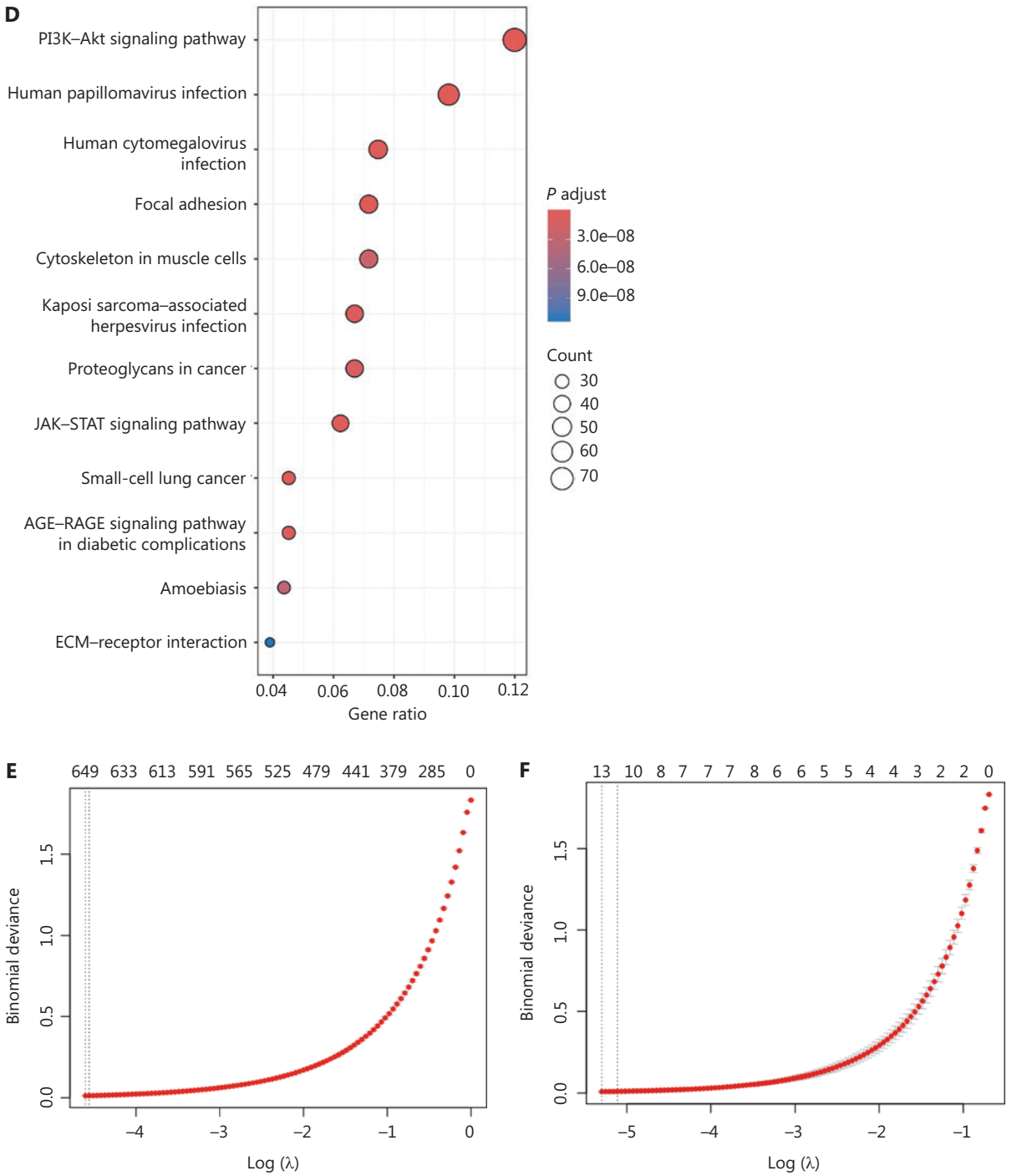


Figure 1 Continued

Methylation of DNA and RNA, especially 5mC and m^{6}A, has a pivotal role in various BPs. Large-scale analyses of 11,080 samples from 33 human cancer types demonstrated that most regulators of 5mC and m^{6}A modifications exhibit similar expression patterns and extensive regulatory interactions[34,35], indicating cooperative involvement in cancer development and potential reciprocal regulation.

Twenty well-recognized 5mC- and 25 m^{6}A-related genes were identified through a literature review to further explore the epigenetic genes influencing *DDR1* expression. Expression data for these genes were extracted from the RNA-seq dataset and visualized as heatmaps (**Figure 2A, B**). Co-expression analysis showed that *DDR1* exhibited the strongest positive correlation with the 5mC regulator, DNMT3A (**Figure 2C**),

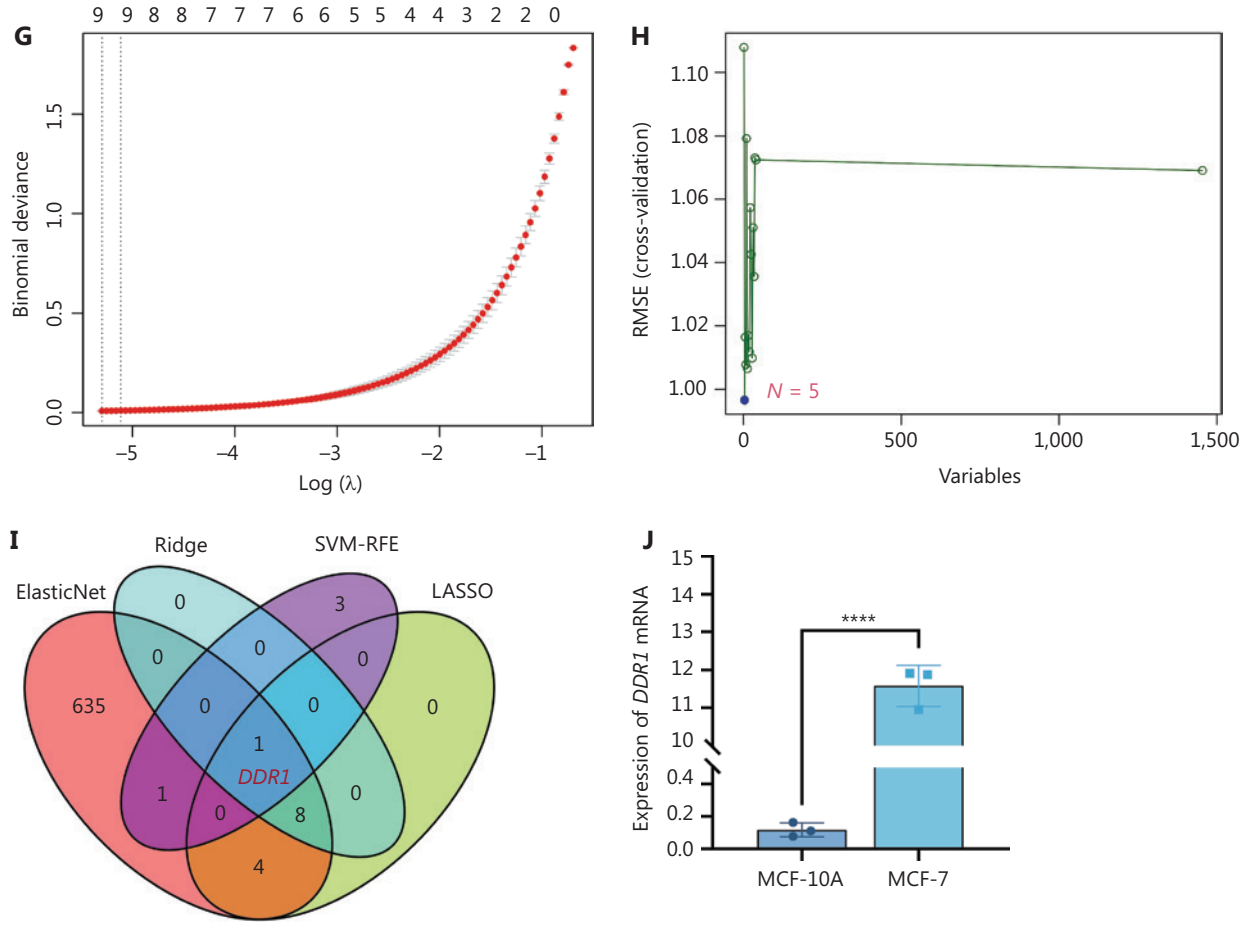


Figure 1 Identifying key DEGs in breast cancer *via* RNA-seq and multiple machine learning algorithms. (A) Workflow of differential gene expression analysis between MCF-10A and MCF-7 cells based on RNA-seq; (B) Volcano plot of DEGs analyzed using the limma package; green indicates downregulated genes, purple indicates upregulated genes (|log2FC| > 3, adj. *P* Value < 0.05); (C) GO enrichment analysis of significantly enriched BP, MF, and CC; (D) KEGG pathway enrichment analysis of DEGs; (E–G) Screening of DEGs using ElasticNet, LASSO, and Ridge algorithms, respectively; (H) Screening results using the SVM-RFE algorithm; (I) Intersection analysis of key genes identified by the four machine learning algorithms (ElasticNet, Ridge, SVM-RFE, and LASSO). Only *DDR1* was consistently selected by all four methods; (J) *DDR1* expression in MCF-7 and MCF-10A cells, derived from RNA-seq data. Data are presented as the mean ± standard deviation (mean ± SD). **** indicates *P* < 0.0001.

and the m^{6}A regulator, METTL7A (**Figure 2D**). Furthermore, multiple potential m^{6}A modification sites on *DDR1* mRNA were predicted using the SRAMP database (**Figure 2E, F**).

The pivotal role of *DDR1* in breast cancer was established through these analyses, revealing likely regulation by the epigenetic modifiers, DNMT3A and METTL7A.

DNA methyltransferase 3A and methyltransferase-like 7A collaborate to regulate discoidin domain receptor 1 and activate breast cancer signaling pathways

Overexpressing DNMT3A or METTL7A cell lines were constructed in MCF-7 cells *via* lentiviral transduction to determine how DNMT3A and METTL7A regulate *DDR1* expression through epigenetic modifications (**Figure S1A**).

RT-qPCR and western blot analyses of transduction efficiency revealed significant upregulation of DNMT3A in the oe-DNMT3A group and METTL7A in the oe-METTL7A group with both DNMT3A and METTL7A showing higher expression in the combined oe-DNMT3A+oe-METTL7A group compared to the single overexpression group (**Figure S1B, C**).

Site-specific MeRIP-qPCR revealed significantly increased m^{6}A modification of *DDR1* mRNA in the oe-METTL7A and oe-DNMT3A+oe-METTL7A groups relative to controls, whereas no change was observed in the oe-DNMT3A group (**Figure S1D**). CBS analysis of DNA methylation in the promoter region of *DDR1* revealed significant increases

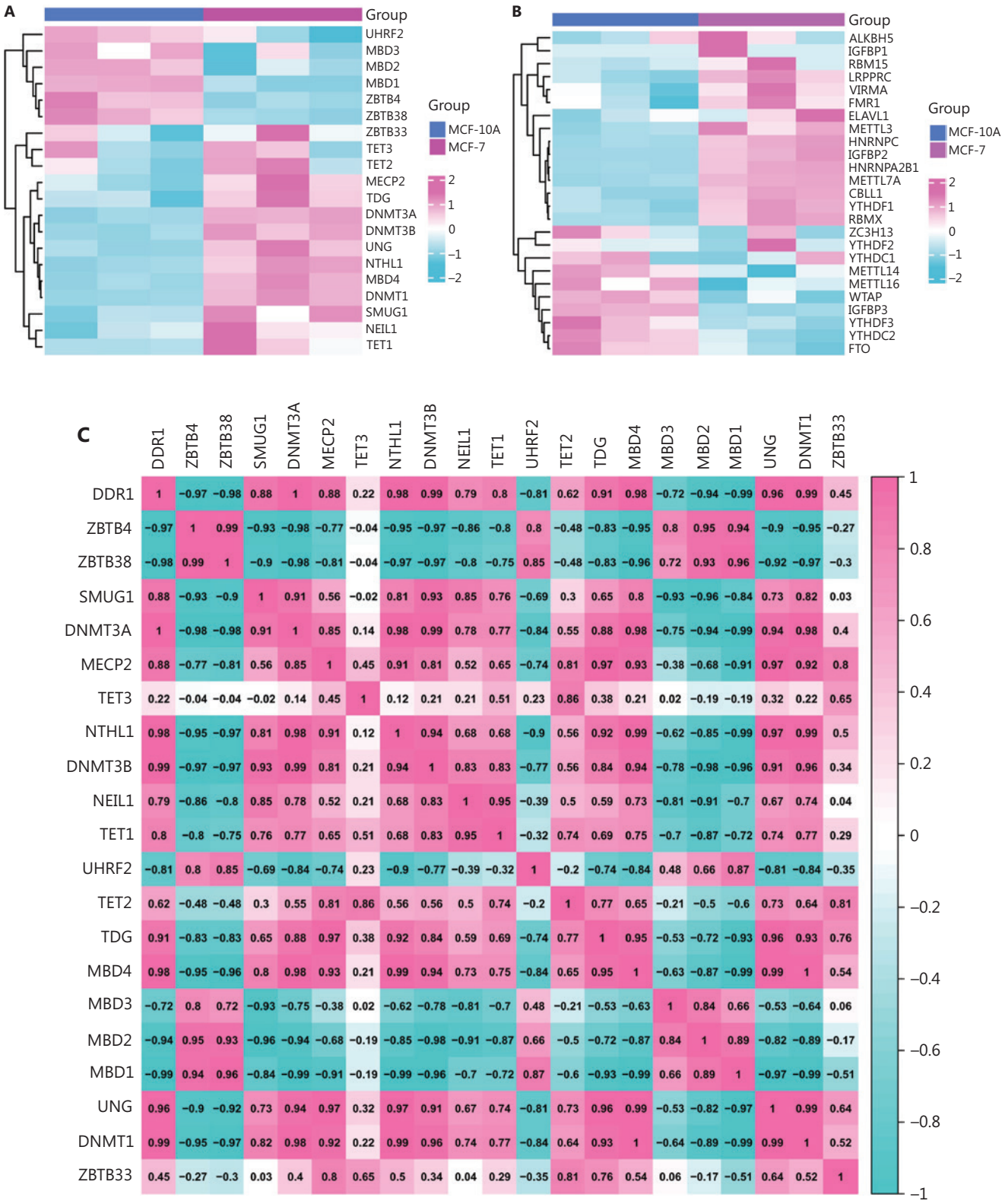


Figure 2 Continued

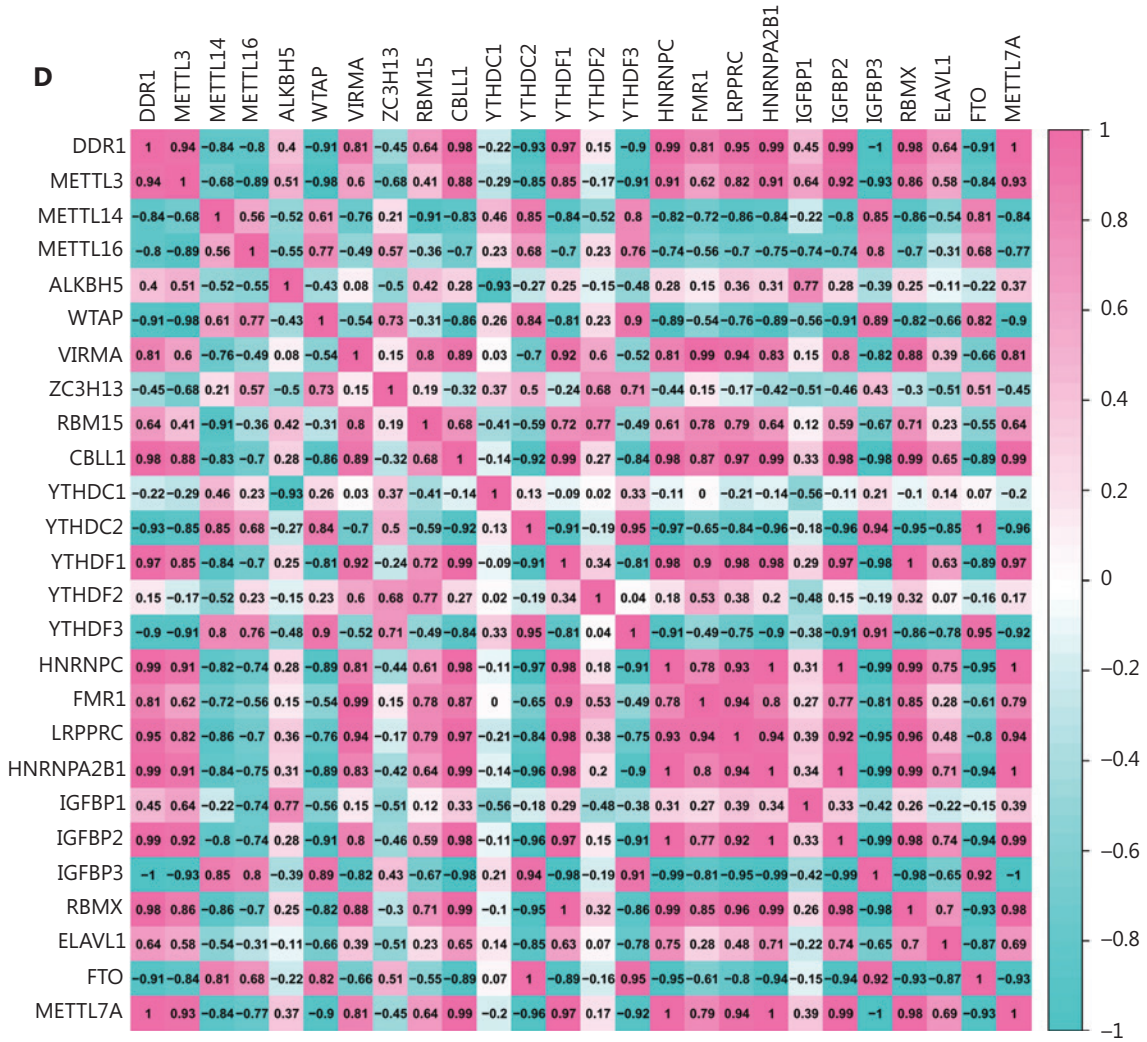


Figure 2 Continued

in methylation levels in both the oe-DNMT3A and oe-DNMT3A+oe-METTL7A groups with no significant change in the oe-METTL7A group (**Figure S1E**). These results indicated that DNMT3A primarily regulates DNA methylation, while METTL7A influences m^{6}A modification, contributing to the epigenetic regulation of *DDR1*.

RNA-seq analysis revealed significant enrichment of DEGs in the JAK-STAT pathway. The effect of *DDR1* on STAT3/CXCL5 signaling was examined given reports that *DDR1* activates STAT3 and promotes CXCL5-mediated neutrophil infiltration and T-cell activation[36-38]. RT-qPCR and western blot showed upregulated DDR1, STAT3, and CXCL5 mRNA/protein levels in the oe-DNMT3A and oe-METTL7A groups compared to controls with the highest levels in the combined overexpression group (**Figure S1F, G**). Co-IP confirmed a DDR1-STAT3 interaction (**Figure S1H**).

These findings demonstrated that DNMT3A and METTL7A collaborate to regulate *DDR1* expression and activate the DDR1/STAT3/CXCL5 axis, potentially influencing the breast cancer microenvironment.

Silencing discoidin domain receptor 1 reverses activation of the breast cancer signaling axis by DNA methyltransferase 3A and methyltransferase-like 7A

Rescue experiments with *DDR1* silencing confirmed that DNMT3A and METTL7A epigenetically regulate *DDR1* expression. First, the silencing efficiency of shRNA targeting *DDR1* was evaluated. RT-qPCR and western blot results demonstrated that sh-DDR1 significantly reduced *DDR1* RNA and protein expression compared to sh-NC and this sequence was selected for subsequent assays (**Figure S2A, B**). DDR1 expression was significantly elevated in the oe-DNMT3A+oe-METTL7A group, whereas co-transfection with

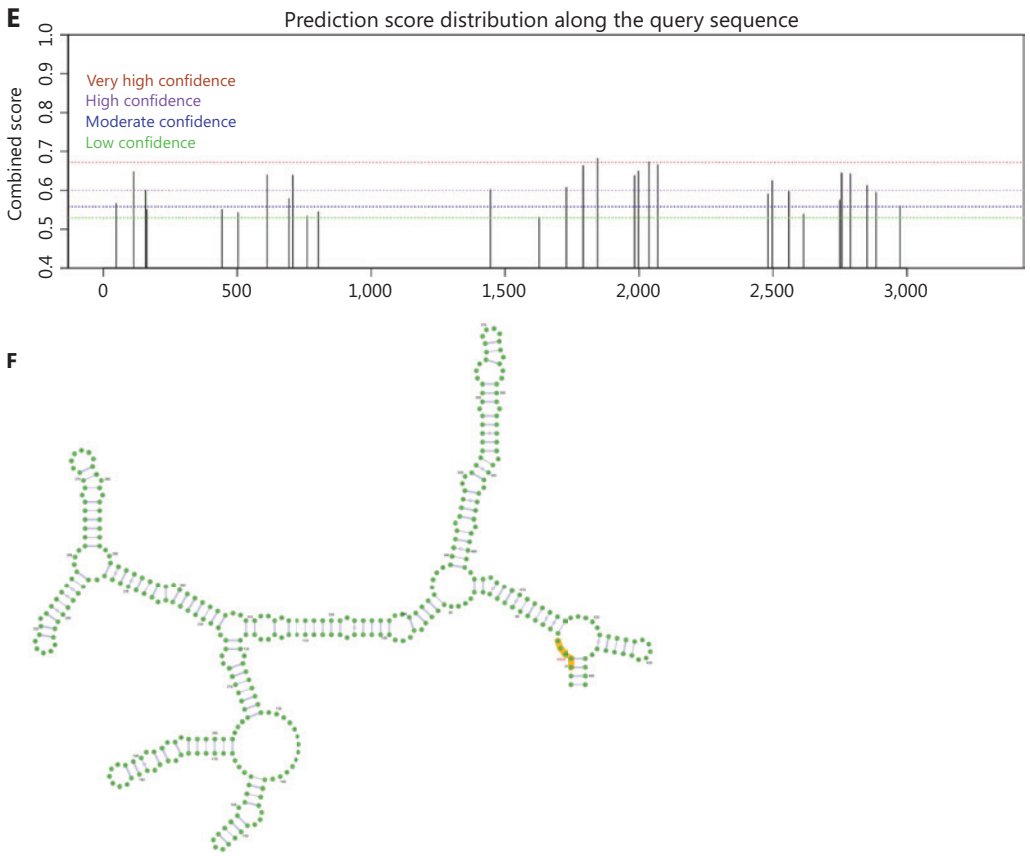


Figure 2 Co-expression analysis of *DDR1* with genes related to 5mC and m^{6}A modifications. (A) Heatmap of 20 5mC-related genes in the RNA-seq dataset; (B) Heatmap of 25 m^{6}A-related genes in the RNA-seq dataset; (C) Co-expression correlation between *DDR1* and 5mC-related genes; (D) Co-expression correlation between *DDR1* and m^{6}A-related genes; (E) Predicted potential m^{6}A modification sites on DDR1 mRNA using the SRAMP database; (F) Distribution of predicted m^{6}A sites on *DDR1* mRNA based on SRAMP analysis.

sh-*DDR1* restored mRNA and protein levels to near-control values (**Figure S3A, B**). These findings demonstrated that *DDR1* knockdown reverses the effects of DNMT3A and METTL7A, supporting the epigenetic co-regulation of *DDR1*.

Further analyses of STAT3 and CXCL5 mRNA and protein levels by RT-qPCR and western blot showed significant upregulation in the oe-DNMT3A+oe-METTL7A group compared to the control group, while significant downregulation was observed in the oe-DNMT3A+oe-METTL7A+sh-*DDR1* group with no significant difference from the control group (**Figure S3C, D**). In the absence of DNMT3A or METTL7A overexpression *DDR1* knockdown alone significantly decreased STAT3 and CXCL5 expression at both the mRNA and protein levels compared to the sh-NC group (**Figure S2C, D**). These results demonstrated that *DDR1* silencing effectively blocked activation of the *DDR1/STAT3/CXCL5* axis by DNMT3A and METTL7A, further supporting the central role of *DDR1* in activating this signaling pathway.

Collectively, the findings demonstrated that DNMT3A and METTL7A epigenetically upregulate *DDR1*, thereby activating the *DDR1/STAT3/CXCL5* axis, which may facilitate breast cancer progression and modulate the TME.

DNA methyltransferase 3A and methyltransferase-like 7A collaborate to enhance breast cancer cell proliferation and invasion capabilities

Overexpression models were established *via* lentiviral transduction to investigate the roles of DNMT3A and METTL7A in breast cancer progression. CCK-8 assays revealed that oe-DNMT3A and oe-METTL7A significantly enhanced cell viability with a further increase in the oe-DNMT3A+oe-METTL7A group (**Figure 3A**). EdU staining confirmed higher proliferation rates in the overexpression groups, especially in the combined group (**Figure 3B**). Similarly, clone formation assays showed an increase in the number of colonies in the oe-DNMT3A and oe-METTL7A groups, which was further elevated in the dual-overexpression group (**Figure**

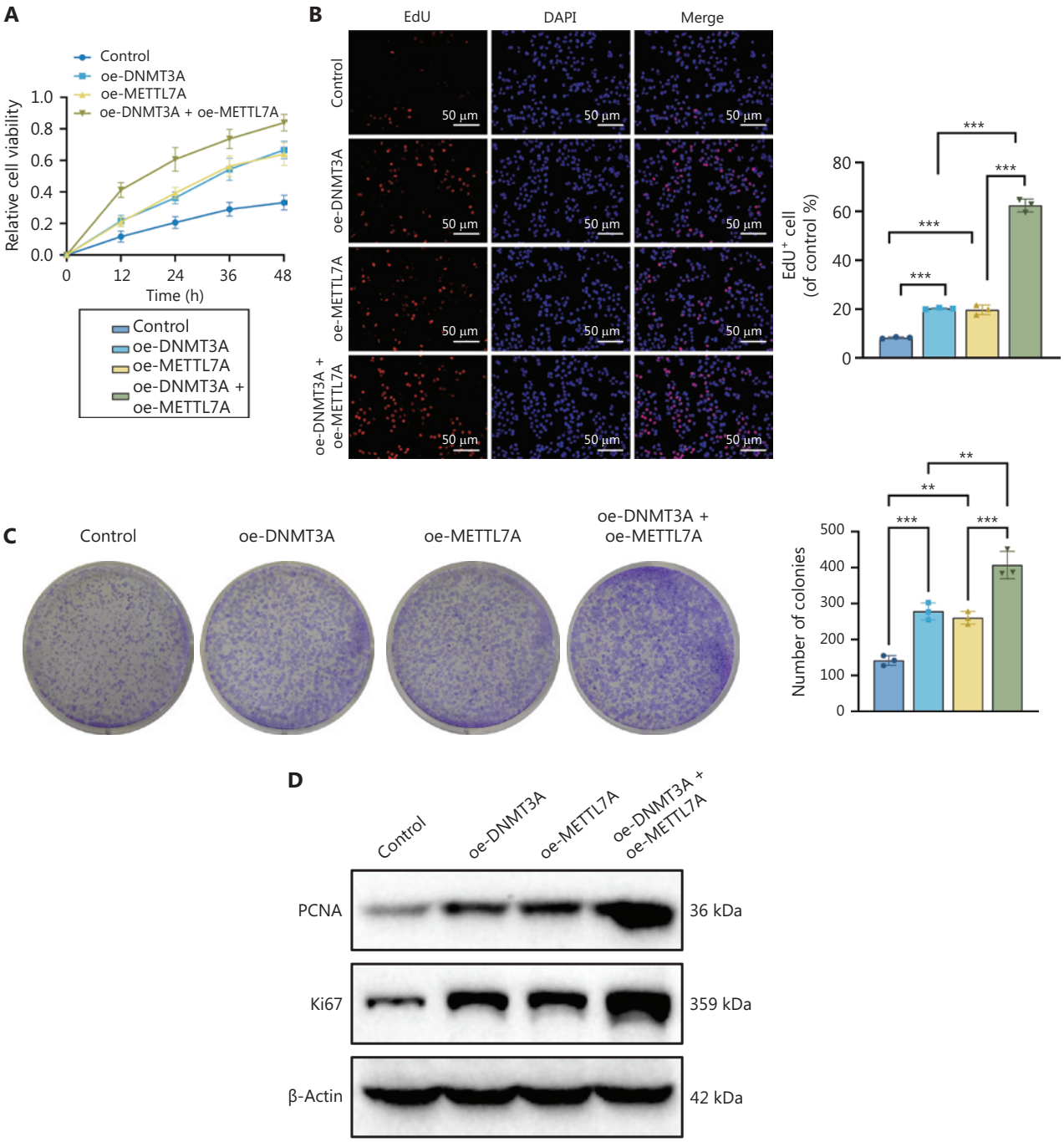


Figure 3 Continued

3C). Western blot analysis revealed upregulated proliferation markers (Ki67 and PCNA) in all overexpression groups with the highest expression occurring in the combined group (**Figure 3D**).

Scratch and Transwell assays demonstrated that both oe-DNMT3A and oe-METTL7A enhanced cell migration and invasion compared to controls with further increases in the combined oe-DNMT3A+oe-METTL7A group (**Figure 3E, F**). Western blot showed corresponding E-cadherin downregulation and MMP-9 upregulation in the oe-DNMT3A and oe-METTL7A groups with more pronounced changes in the dual-overexpression group (**Figure 3G**).

These findings indicated that DNMT3A and METTL7A markedly promote breast cancer cell proliferation, migration, and invasion with synergistic effects when co-expressed, likely through coordinated regulation of key signaling pathways.

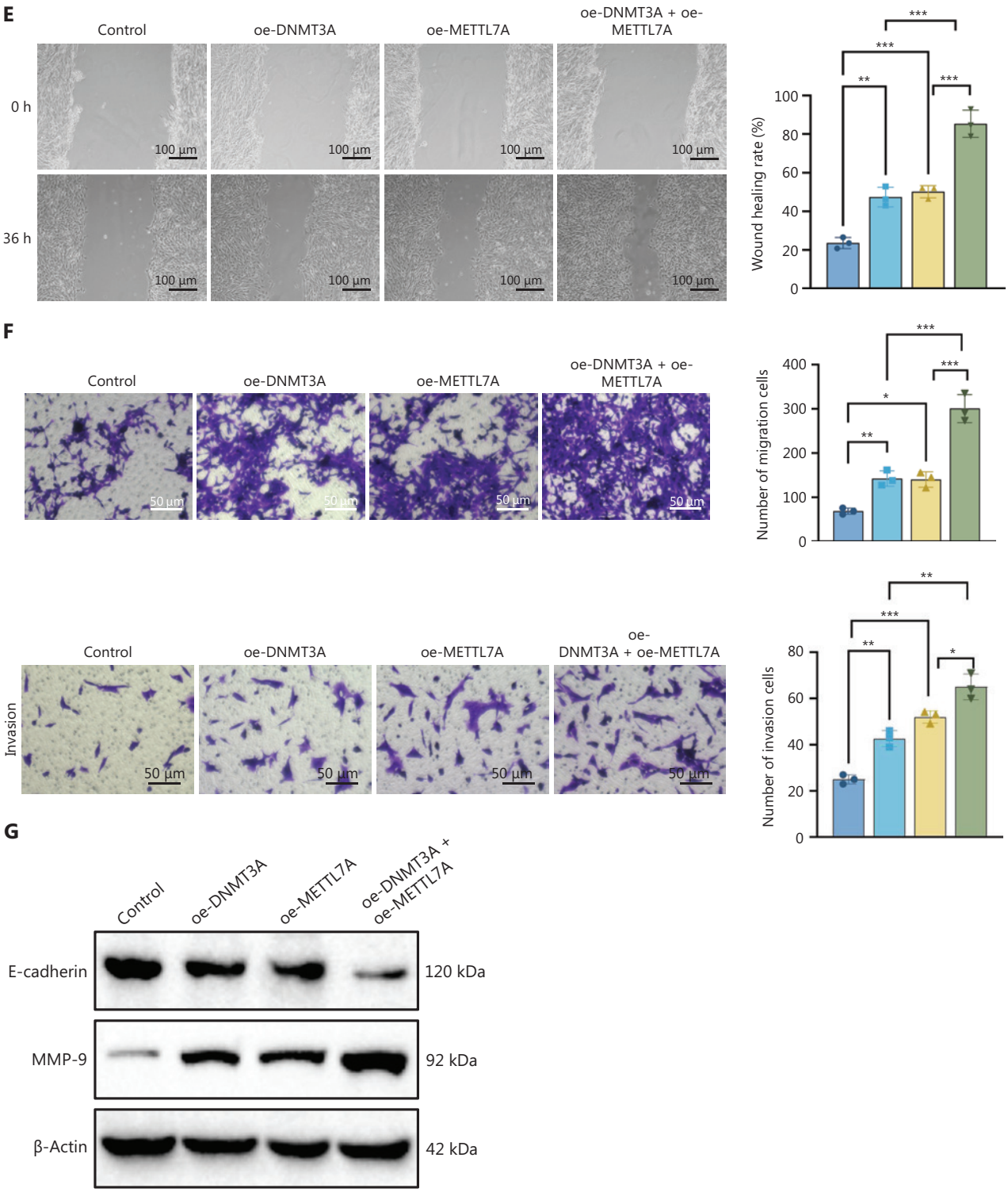


Figure 3 DNMT3A and METTL7A synergistically promote breast cancer cell proliferation and migration. (A) CCK-8 assay for cell viability; (B) EdU staining assay to assess cell proliferation; (C) Colony formation assay to evaluate clonogenic capacity; (D) Western blot analysis of proliferation markers (Ki67 and PCNA); (E) Scratch wound assay to assess cell migration; (F) Transwell and invasion assay to evaluate invasive capacity; (G) Western blot analysis of migration and invasion markers (E-cadherin and MMP-9). All experiments were performed in triplicate. Multiple-group comparisons were performed using one-way ANOVA, and data from different time points were analyzed using two-way ANOVA. Data are expressed as the mean ± SD. *P < 0.05, **P < 0.01, ***P < 0.001, ****P < 0.0001.

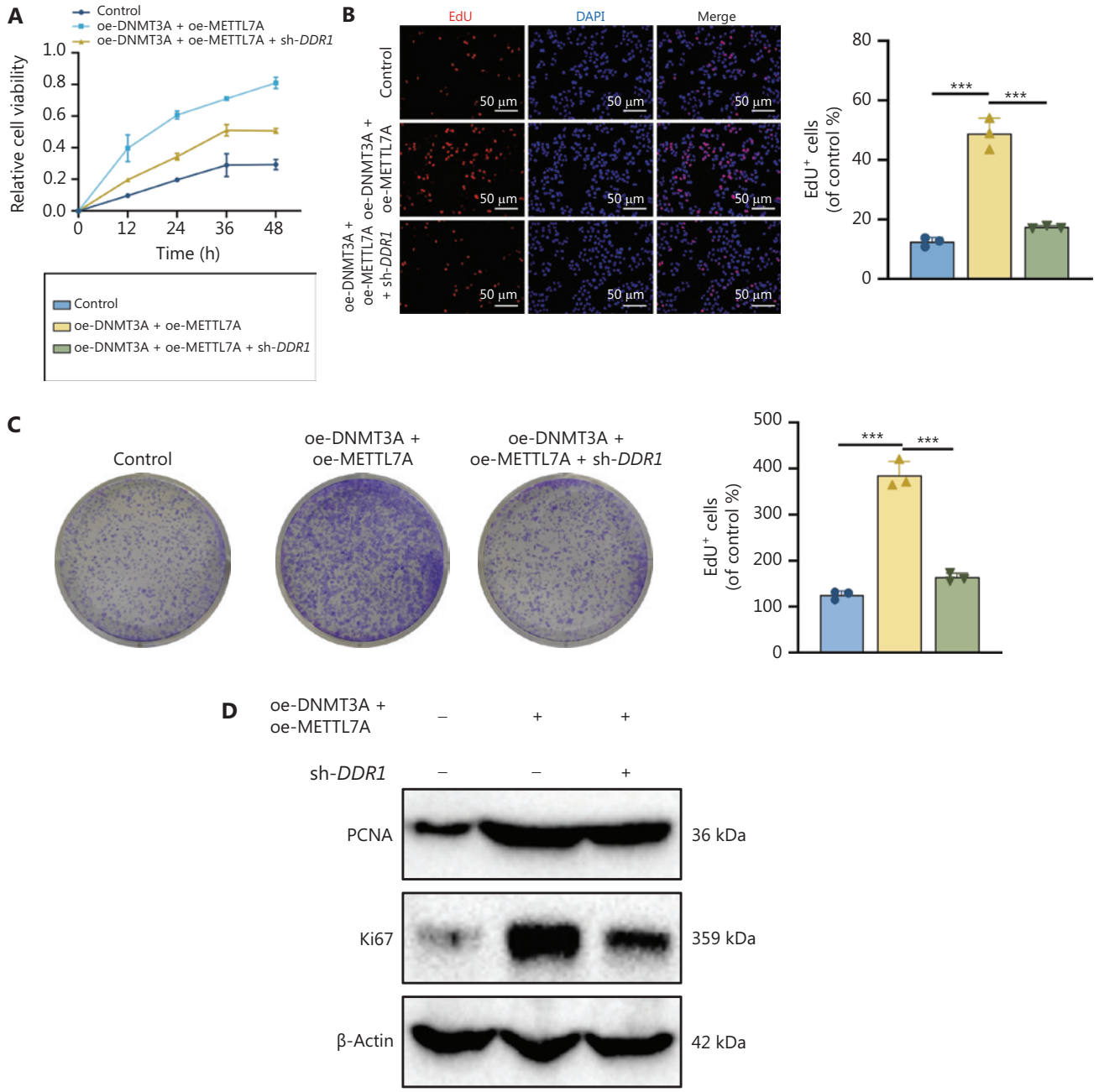


Figure 4 Continued

Silencing discoidin domain receptor 1 significantly suppresses the proliferative and invasive effects of DNA methyltransferase 3A and methyltransferase-like 7A in breast cancer cells

A rescue experiment was performed by silencing *DDR1* to assess the pivotal role of *DDR1* in mediating the proliferative and migratory effects of DNMT3A and METTL7A.

CCK-8 assays showed higher cell viability in the oe-DNMT3A+oe-METTL7A group *versus* controls, which was reversed by *DDR1* knockdown (oe-DNMT3A+oe-METTL7A+sh-*DDR1*; **Figure 4A**). EdU staining revealed a higher proportion of EdU$^+$ cells in the oe-DNMT3A+oe-METTL7A group that was reduced upon *DDR1* silencing (**Figure 4B**). Colony formation assays showed similar trends with an elevated number of colonies in the dual-overexpression group and a significant reduction after *DDR1* knockdown (**Figure 4C**). Western blot analysis confirmed upregulation of Ki67

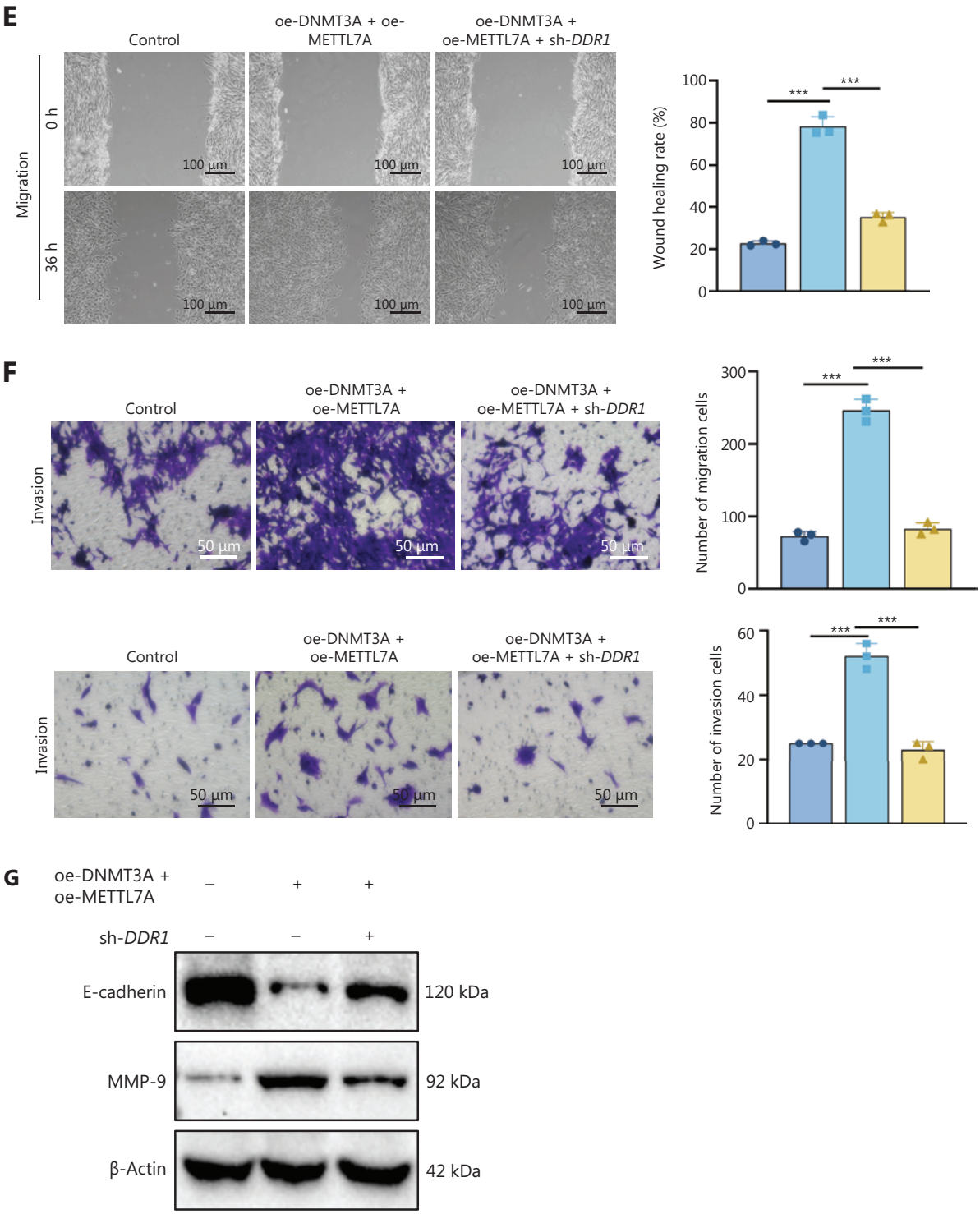


Figure 4 Silencing *DDR1* suppresses DNMT3A- and METTL7A-induced proliferation and migration of breast cancer cells. (A) CCK-8 assay for cell viability; (B) EdU staining assay to assess cell proliferation; (C) Colony formation assay to evaluate clonogenic capacity; (D) Western blot analysis of proliferation markers (Ki67 and PCNA); (E) Scratch wound assay to assess cell migration; (F) Transwell and invasion assay to evaluate invasive capacity; (G) Western blot analysis of migration and invasion markers (E-cadherin and MMP-9). All experiments were performed in triplicate. Multiple-group comparisons were performed using one-way ANOVA and data from different time points were analyzed using two-way ANOVA. Data are expressed as the mean ± SD. **P* < 0.05, ***P* < 0.01, ****P* < 0.001, *****P* < 0.0001.

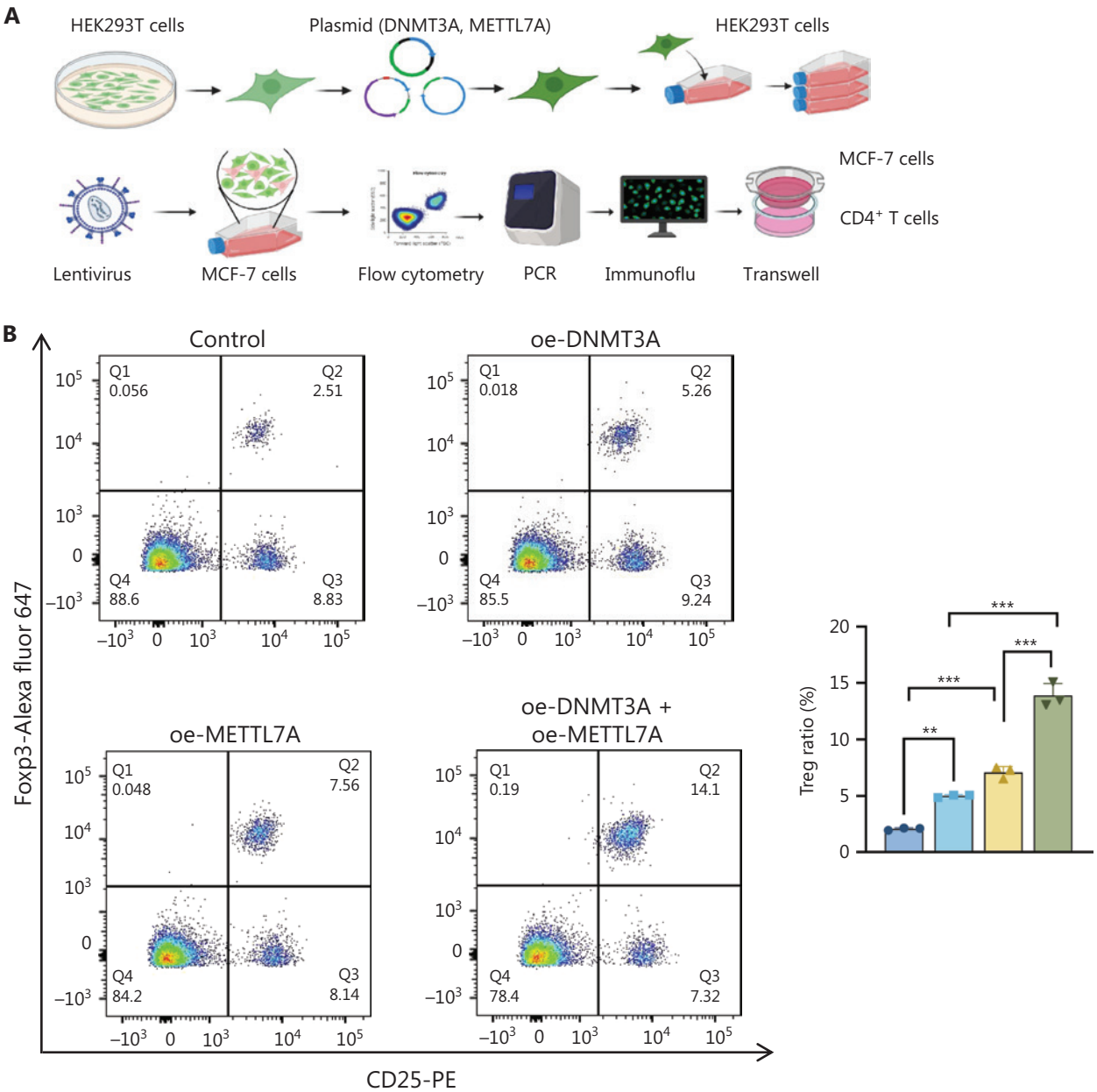


Figure 5 Continued

and PCNA in the oe-DNMT3A+oe-METTL7A group, which was markedly decreased by DDR1 silencing (**Figure 4D**).

The scratch assay demonstrated a significantly greater migration distance in the oe-DNMT3A+oe-METTL7A group compared to controls, which was markedly reduced by *DDR1* knockdown (**Figure 4E**). Transwell migration and invasion assays further showed that the number of cells was substantially higher in the dual-overexpression group, whereas *DDR1* silencing suppressed both migration and invasion (**Figure 4F**). Western blot analysis of migration and invasion markers revealed that E-cadherin was significantly downregulated and MMP-9 significantly upregulated in the oe-DNMT3A+oe-METTL7A group. However, silencing DDR1 reversed these effects, leading to upregulation of E-cadherin and downregulation of MMP-9 (**Figure 4G**).

These findings highlight the essential role of *DDR1* in mediating the cooperative effects of DNMT3A and METTL7A on breast cancer cell proliferation, migration, and invasion with *DDR1* silencing effectively abolishing the synergistic activity and underscoring the potential as a therapeutic target.

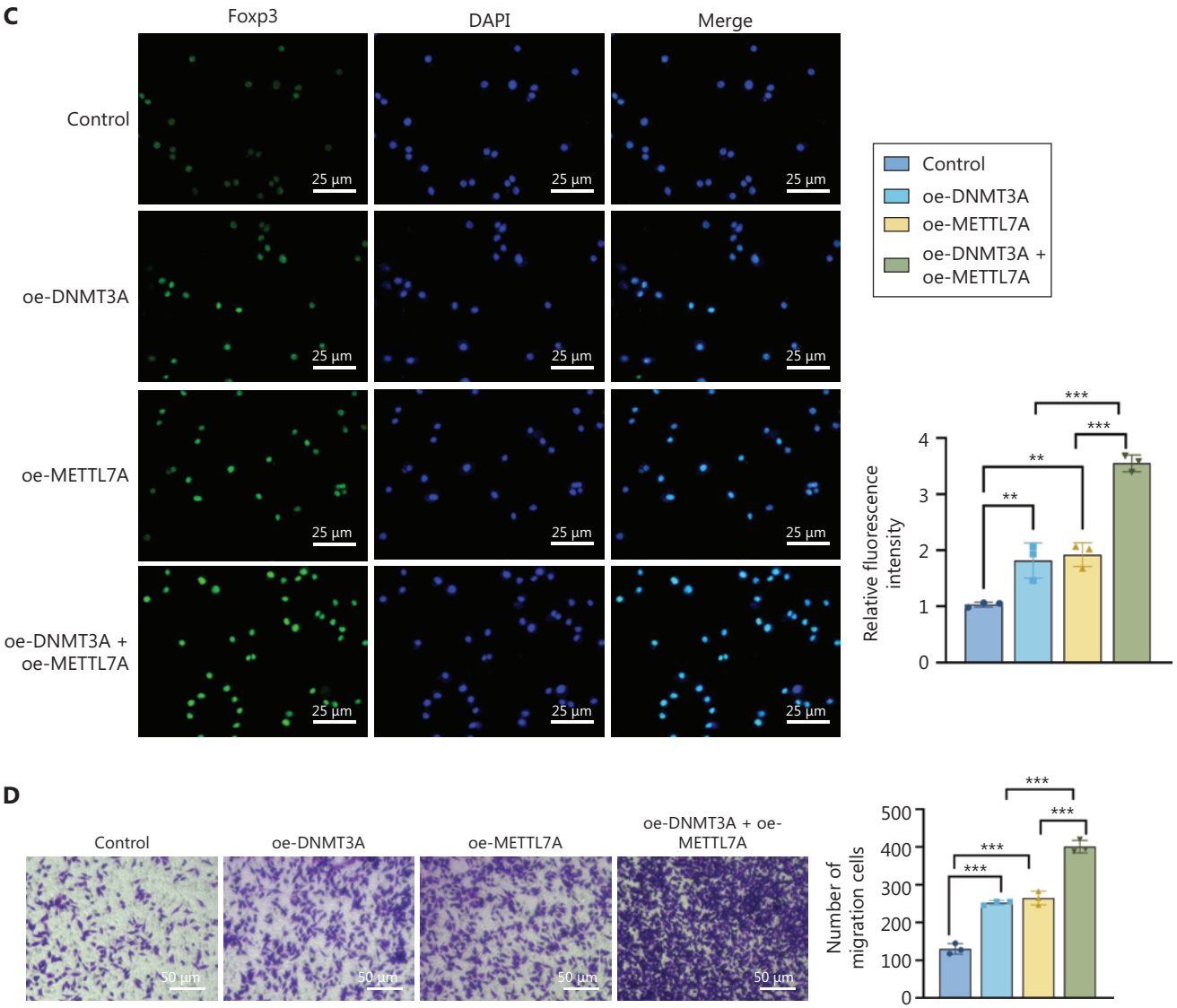


Figure 5 The DDR1/STAT3/CXCL5 axis promotes Treg differentiation and migration induced by breast cancer cells. (A) Schematic of the experimental design; (B) Flow cytometry analysis of Treg proportions ($CD4^+CD25^+Foxp3^+$); (C) Immunofluorescence staining of the Treg marker, Foxp3; (D) Transwell assay assessing the migration capacity of Tregs. All experiments were performed in triplicate. Data are expressed as the mean ± SD. Multiple-group comparisons were performed using one-way ANOVA. *P < 0.05, **P < 0.01, ***P < 0.001, ****P < 0.0001.

The discoidin domain receptor 1 / signal transducer and activator of transcription 3 / C-X-C motif chemokine ligand 5 axis promotes regulatory T cell differentiation and migration induced by breast cancer cells

DDR1 and CXCL5 have been shown to induce NET formation, thereby promoting Treg immune infiltration and driving tumor growth and metastasis[32]. Breast cancer cell lines overexpressing DNMT3A and METTL7A were established *via* lentiviral transduction to investigate the role of the DDR1/STAT3/CXCL5 axis in regulating Treg differentiation and migration. These cells were then co-cultured with human $CD4^+$ T cells, as illustrated in the experimental workflow (**Figure 5A**).

Flow cytometry analysis of Treg cell proportions ($CD4^+CD25^+Foxp3^+$) revealed that both the oe-DNMT3A and oe-METTL7A groups exhibited significantly increased Treg ratios compared to the control group with the highest proportion in the oe-DNMT3A+oe-METTL7A group (**Figure 5B**). Immunofluorescence staining showed a marked upregulation of the Treg marker, Foxp3, in both single overexpression

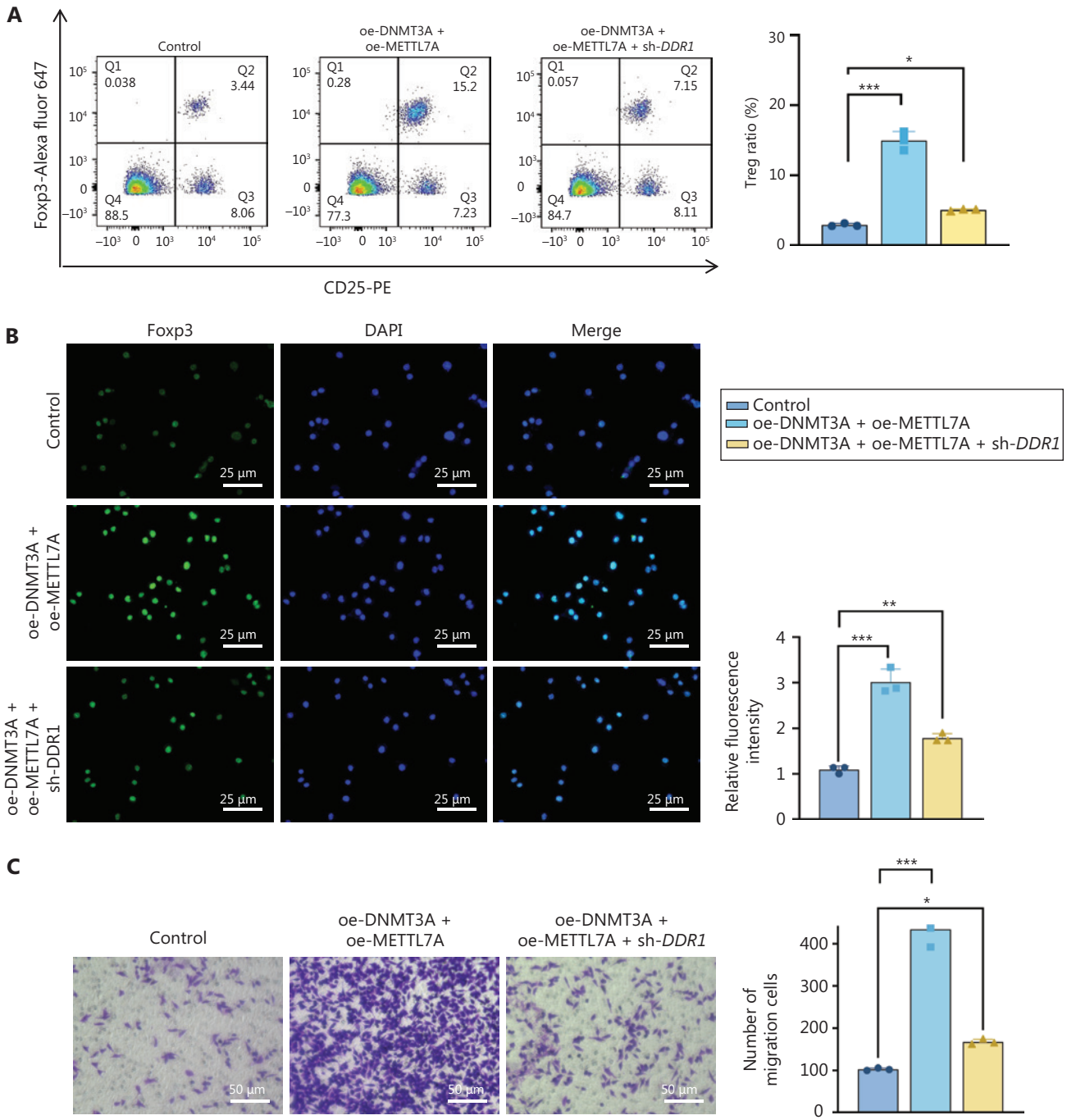


Figure 6 Silencing *DDR1* suppresses the ability of breast cancer cells to induce Treg differentiation and migration. (A) Flow cytometry analysis of Treg proportions ($CD4^+CD25^+Foxp3^+$); (B) Immunofluorescence staining of the Treg marker, Foxp3; (C) Transwell assay assessing Treg migration. All experiments were performed in triplicate. Data are expressed as the mean ± SD. Multiple-group comparisons were performed using one-way ANOVA. *P < 0.05, **P < 0.01, ***P < 0.001, ****P < 0.0001.

groups with even higher expression in the combined overexpression group (**Figure 5C**). These results suggested that the DDR1/STAT3/CXCL5 axis may synergistically promote Treg differentiation in the context of breast cancer.

To assess the ability of breast cancer cells to induce Treg migration, a Transwell assay was performed using conditioned media from the different groups. Both oe-DNMT3A and oe-METTL7A groups exhibited significantly enhanced Treg

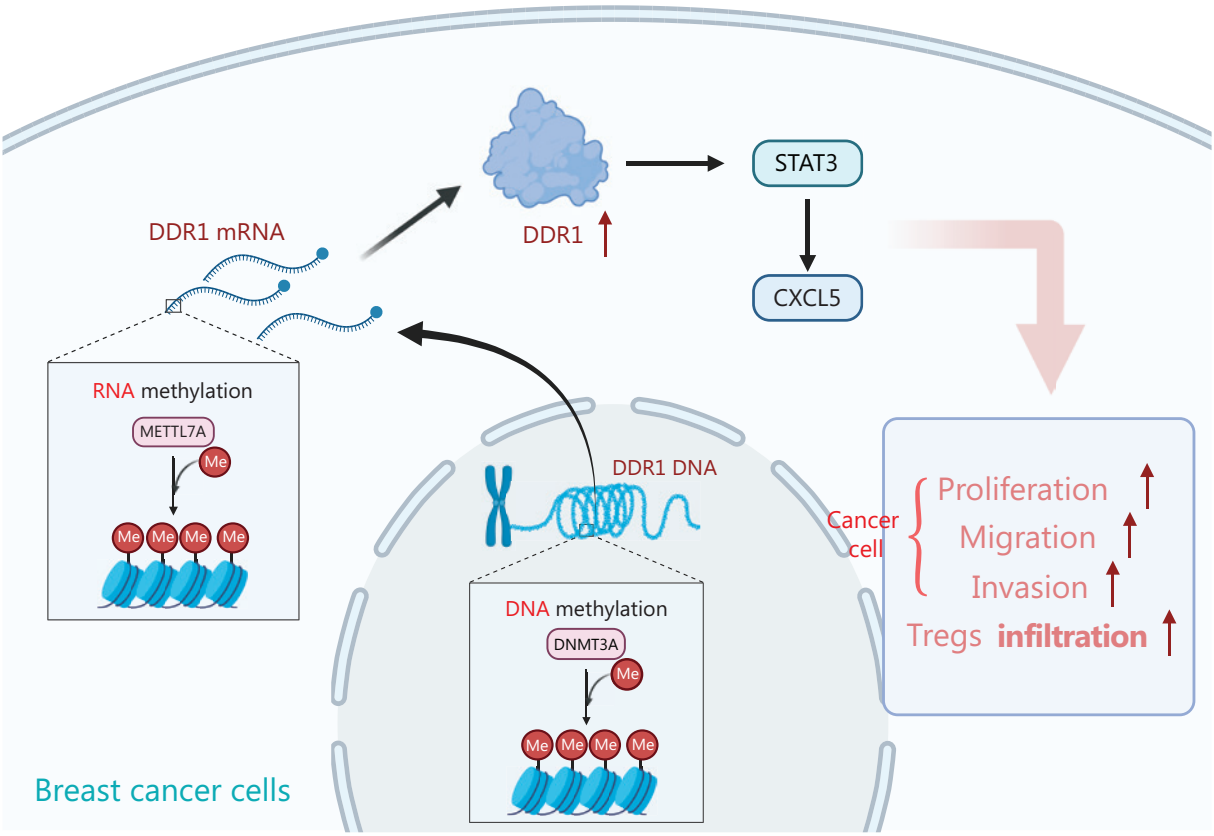


Figure 7 Schematic illustration of the molecular mechanism by which DNMT3A and METTL7A co-regulate the *DDR1/STAT3/CXCL5* axis, promoting Treg infiltration and contributing to breast cancer recurrence. This study elucidated a synergistic epigenetic regulatory network where DNMT3A (DNA methylation) and METTL7A (m6A modification) co-upregulate *DDR1*, activating the *DDR1/STAT3/CXCL5* axis to promote Treg infiltration, immunosuppression, and tumor recurrence. DNMT3A-mediated promoter methylation enhances DDR1 transcription, while METTL7A stabilizes *DDR1* mRNA *via* m6A modification, forming a "DNA-RNA dual modification" mechanism. Activated *DDR1* recruits STAT3 to upregulate CXCL5, directing regulatory T cell (Treg) recruitment *via* CXCR2 signaling, which suppresses anti-tumor immunity and fosters an immunosilent niche for cancer progression. Combined DNMT3A/METTL7A overexpression synergistically potentiates tumor proliferation, migration, and recurrence *in vivo*, while *DDR1* silencing disrupts this axis, reversing immunosuppression and tumor growth. The DNMT3A-METTL7A-DDR1 signature holds promise as a biomarker for recurrence prediction and therapeutic targeting, offering a novel framework for precision immunotherapy in breast cancer. CXCL5, C-X-C motif chemokine ligand 5; *DDR1*, discoidin domain receptor 1; METTL7A, methyltransferase-like 7A; m6A, N6-methyladenosine; STAT3, signal transducer and activator of transcription 3; Treg, regulatory T cell.

migration relative to the control with further enhancement observed in the oe-DNMT3A+oe-METTL7A group (**Figure 5D**). These results indicate that the *DDR1/STAT3/CXCL5* axis promotes Treg migration by stimulating CXCL5 secretion.

Collectively, the *DDR1/STAT3/CXCL5* signaling axis markedly promotes Treg differentiation and migration with these effects amplified by the cooperative activity of DNMT3A and METTL7A. These findings provided critical evidence for understanding the regulatory mechanisms of the breast cancer immune microenvironment.

Silencing discoidin domain receptor 1 significantly suppresses the ability of breast cancer cells to induce regulatory T cell differentiation and migration

Rescue experiments with *DDR1* knockdown demonstrated the essential role in DNMT3A/METTL7A-driven Treg induction. Flow cytometry analysis revealed a marked increase in $CD4^+CD25^+Foxp3^+$ Tregs in the oe-DNMT3A+oe-METTL7A

group, which was significantly reduced following *DDR1* silencing (oe-DNMT3A+oe-METTL7A+sh-*DDR1*; **Figure 6A**). Immunofluorescence staining confirmed elevated Foxp3 expression in the combined overexpression group with substantial attenuation upon *DDR1* knockdown (**Figure 6B**), indicating *DDR1* is essential for Treg differentiation in this axis.

A Transwell chemotaxis assay was performed using conditioned media to assess the effect of *DDR1* on Treg migration. The results demonstrated that Treg migratory capacity was enhanced in the oe-DNMT3A+oe-METTL7A group relative to controls, whereas *DDR1* knockdown substantially reduced this effect (**Figure 6C**). These results suggested that CXCL5, acting through activation of the DDR1/STAT3 axis, markedly enhances Treg chemotaxis, an effect that can be effectively reversed by *DDR1* silencing.

In conclusion, *DDR1* facilitated Treg differentiation and migration in the breast cancer microenvironment. *DDR1* silencing effectively inhibited the immunoregulatory effects of DNMT3A and METTL7A, providing important mechanistic insights into the epigenetic regulation of tumor immune evasion in breast cancer.

DNA methyltransferase 3A and methyltransferase-like 7A synergistically promote breast cancer growth, recurrence, and immune microenvironment modulation

The *in vivo* roles of DNMT3A and METTL7A in breast cancer recurrence and modulation of the immune microenvironment were examined using a nude mouse xenograft model, followed by molecular and histologic analyses, as outlined in the experimental workflow (**Figure S4A**).

Tumor volumes increased significantly in the oe-DNMT3A and oe-METTL7A groups relative to controls with the greatest increase observed in the oe-DNMT3A+oe-METTL7A group (**Figure S4B**). The excised tumors in these groups exhibited higher weights after 28 d, especially in the combined overexpression group (**Figure S4C, D**). Additionally, the oe-DNMT3A+oe-METTL7A group displayed accelerated recurrence and higher recurrence rates (**Figure S4E**), indicating that DNMT3A and METTL7A synergistically promote breast cancer growth and recurrence.

Immunohistochemistry (IHC) analyses revealed significantly increased expression of DDR1, STAT3, and CXCL5 in tumor tissues from the oe-DNMT3A and oe-METTL7A groups compared to controls with further upregulation in the combined overexpression group (**Figure S4F**). Flow cytometry demonstrated a significantly higher proportion of Tregs in tumor tissues from the oe-DNMT3A and oe-METTL7A groups with the highest proportion in the combined group (**Figure S4G**). Immunofluorescence staining for Cit-H3 and DNA further showed that NET formation was markedly enhanced in the oe-DNMT3A and oe-METTL7A groups and significantly elevated in the combined group (**Figure S4H**).

Collectively, these findings indicated that DNMT3A and METTL7A promote breast cancer growth, recurrence, and immune microenvironment remodeling through activation of the DDR1/STAT3/CXCL5 axis, thereby enhancing Treg infiltration and NETs formation. This study provided new evidence supporting the molecular mechanisms underlying breast cancer progression.

Silencing *DDR1* attenuates DNMT3A- and METTL7A-mediated breast cancer recurrence and immune microenvironment modulation

A rescue experiment involving *DDR1* silencing was performed to verify the critical role of *DDR1* in DNMT3A- and METTL7A-mediated breast cancer recurrence and immune microenvironment regulation. Tumor growth, recurrence, and related molecular markers were subsequently analyzed, as outlined in the experimental design (**Figure S5A**).

Tumor volume and weight were significantly increased in the oe-DNMT3A+oe-METTL7A group compared to controls, whereas *DDR1* knockdown (sh-*DDR1*) reversed these effects (**Figure S5B–D**). Recurrence rates were elevated and recurrence times shortened in the oe-DNMT3A+oe-METTL7A group, but both parameters were suppressed by *DDR1* silencing (**Figure S5E**). These results indicated that *DDR1* is critical for DNMT3A/METTL7A-mediated tumor growth and recurrence.

IHC staining showed elevated DDR1, STAT3, and CXCL5 expression in the oe-DNMT3A+oe-METTL7A group relative to controls, which was reduced following *DDR1* knockdown (**Figure S5F**). Flow cytometry revealed increased Treg infiltration in the oe-DNMT3A+oe-METTL7A group, an effect reversed by DDR1 silencing (**Figure S5G**). Immunofluorescence demonstrated enhanced NET formation (Cit-H3/DNA co-localization) in the oe-DNMT3A+oe-METTL7A group, while DDR1 silencing suppressed NETs (**Figure S5H**).

Taken together, these results demonstrated that *DDR1* silencing significantly impairs the ability of DNMT3A and METTL7A to promote breast cancer recurrence and modulate the immune microenvironment, supporting *DDR1* as a promising therapeutic target in breast cancer.

Discussion

This study identified a novel "dual epigenetic modification" mechanism in which DNMT3A and METTL7A cooperate to regulate *DDR1* expression. Mechanistic evidence indicated that METTL3 ablation reduces m6A modification of DNMT3A mRNA, thereby impairing YTHDF1-mediated

translation of DNMT3A[39]. Long-term ectoine treatment in HaCaT cells modulates Dnmt1, Dnmt3a, and Mettl14 mRNA levels, induces mild DNA demethylation, alters the expression of epigenetic regulators, and reduces cell proliferation[40]. Furthermore, METTL3-METTL14 has been reported to recruit DNMT1 to chromatin for gene-body methylation[41]. While DNMT3A promotes *DDR1* transcription *via* promoter methylation, METTL7A stabilizes *DDR1* mRNA through m6A modification[42,43]. Unlike classical m6A writers (e.g., METTL3), METTL7A exhibits distinct substrate specificity. Co-IP data further confirmed the physical interaction between DDR1 and STAT3, suggesting a potential regulatory complex. The findings deepen understanding of epigenetic crosstalk and reveal a multilayered co-regulatory network that extends beyond single-modification paradigms.

DDR1 inhibitors (e.g., 7rh) block breast cancer metastasis by targeting collagen signaling, whereas STAT3 inhibitors (e.g., Stattic) modulate cancer stem cell phenotypes[44,45]. CXCL5, which acts *via* CXCR2, recruits MDSCs and the CXCL5 inhibitor, reparixin, has entered clinical trials[21,46]. In the present study activation of the *DDR1/STAT3/CXCL5* axis promoted Treg infiltration. Single-cell RNA-seq and flow cytometry analyses demonstrated that CXCL5 preferentially recruits Tregs over other immunosuppressive cells. TCGA data further linked elevated *DDR1* expression to poor breast cancer prognosis with weaker associations observed in other cancers, indicating tissue-specific effects[32,47]. Unlike CCL22/CCR4-mediated Treg recruitment, CXCL5 was elevated in recurrent than primary tumors, indicating a predominant role during recurrence. These findings reveal spatiotemporal heterogeneity in immune evasion.

Previous studies have shown that DNA methyltransferase inhibitors (e.g., 5-Aza) reverse immunosuppression in breast cancer, while m6A regulators, like the METTL3 inhibitor, STM2457, enhance anti-tumor immunity[48-50]. *DDR1* inhibitors (e.g., 7rh) also exhibit anti-metastatic effects[51,52]. The present study identified the DNMT3A-METTL7A-*DDR1* axis as a driver of Treg enrichment in recurrent breast cancer. *DDR1* knockdown significantly reduced the proportion of Tregs *in vivo*. Treg infiltration may dominate immunosuppression in recurrence compared to PD-L1/PD-1-mediated exhaustion, suggesting that tumors adapt *via* epigenetic mechanisms under therapy. Future studies should explore how different treatments modulate this axis to optimize combinations.

Machine learning algorithms, including LASSO and SVM-RFE, have proven effective in biomarker discovery for breast cancer, such as predicting trastuzumab response in HER2-positive patients[53,54]. Multi-omics tools, such as MOFA+, have further enabled molecular subtyping and target identification[55,56]. In the present study LASSO, Ridge, SVM-RFE, and ElasticNet were applied, leading to the identification of *DDR1* as a key regulator. Although these approaches surpass traditional differential expression analysis in reducing false-positives and capturing gene–gene interactions, the mechanistic relationship between *DDR1* and Treg infiltration remains unresolved, underscoring the inherent "black box" limitation. Future investigations should integrate multi-omics datasets to improve both predictive accuracy and mechanistic interpretation.

Epigenetic therapies, like the DNMT inhibitor, decitabine, have been shown to modulate the TIME, thereby enhancing the efficacy of breast cancer treatment[57,58]. Preclinical studies indicate that *DDR1* inhibitors, including 7rh, effectively suppress TNBC metastasis[59-61]. Clinically, DNMT3A/METTL7A-*DDR1* axis activation correlates with poor prognosis, suggesting utility as a liquid biopsy biomarker[62]. Therapeutically, *DDR1* inhibition reduces Treg infiltration, while CXCL5-neutralizing antibodies may synergize with PD-1 blockade[24,32]. However, current DNMT3A inhibitors lack METTL7A targeting[63] and CXCL5 blockade risks autoimmune effects, requiring careful dose optimization[64]. Future clinical trials should stratify patients based on *DDR1* methylation status to guide personalized targeted therapy.

This study highlighted the critical role of the *DDR1/STAT3/CXCL5* axis in breast cancer, but validation across molecular subtypes remains necessary. *In vivo* experiments were conducted in immunodeficient nude mice, which lack mature T-cell populations and do not fully recapitulate the human immune microenvironment. This limitation may hinder a comprehensive assessment of Treg biology. Tregs dynamically interact with effector T cells through multiple mechanisms in an intact immune system, including CTLA-4–mediated dendritic cell regulation and IL-2 consumption[65,66]. Consequently, the relationship between Treg infiltration and therapeutic response should be interpreted with caution. Future studies should incorporate immunocompetent models and clinical samples for validation. The findings also indicated that CXCL5 promotes Tregs *via* CXCR2, although downstream signaling events within Tregs remain incompletely defined. CXCR2 may regulate Treg migration and immunosuppressive activity through PI3K–Akt and MAPK/ERK pathways, warranting further investigation using gene knockout or pharmacologic inhibition[67,68]. Moreover, *DDR1*/CXCL5-induced NET formation has been reported to enhance Treg infiltration and drive tumor progression[32]. Other immune cells within the TME, including neutrophils *via* NETs and MDSCs, may cooperate with Tregs to reinforce immunosuppression, yet the interactions with CXCL5 require further study. Future work should not only verify these mechanisms in clinical specimens and immunocompetent models but also assess the stability of *DDR1*-targeted strategies and explore *DDR1* interactions with additional immune cell subsets to clarify a broader regulatory role in tumor immunity.

Although this study systematically revealed that DNMT3A and METTL7A cooperate to regulate the *DDR1/STAT3/CXCL5* axis through epigenetic modifications to promote Treg infiltration and breast cancer recurrence, we acknowledge that the experimental validation was primarily based on MCF-7

cells (Luminal A subtype). Broader validation in other molecular subtypes, such as TNBC or HER2-positive breast cancer, was not provided, representing a study limitation. However, previous reports have documented *DDR1* overexpression across multiple breast cancer subtypes, where *DDR1* contributes to extracellular matrix remodeling, immune evasion, and enhanced migratory capacity. For example, studies have shown that *DDR1* significantly promotes adhesion and invasion of TNBC cells by enhancing collagen–receptor signaling[69]. These findings support the theoretical applicability of the proposed "DNMT3A/METTL7A–DDR1–STAT3–CXCL5" signaling net-work across different subtypes. Corollary studies will incorporate TNBC (MDA-MB-231) and $HER2^+$ (SK-BR-3) cell models to systematically evaluate the expression and functional consistency of this epigenetic–immune regulatory pathway, thereby improving generalizability and translational potential.

The findings also suggest that epigenetic modifications may exert dynamic regulatory effects on tumor immune evasion, which could vary with disease stage and therapeutic interventions. Future research should investigate how distinct treatment regimens modulate the DNMT3A/METTL7A–*DDR1* axis and explore integration into combination therapy strategies. Specifically, patient stratification based on *DDR1* methylation status may enhance the precision and responsiveness of immunotherapy.

Conclusions

This study elucidated a novel molecular mechanism by which DNMT3A and METTL7A cooperate to regulate *DDR1* expression through epigenetic modifications, triggering activation of the *DDR1/STAT3/CXCL5* signaling axis and promoting breast cancer cell proliferation, migration, invasion, and Treg infiltration. This epigenetic co-regulatory axis has a pivotal role in breast cancer recurrence and immune evasion, enriching our understanding of the regulatory mechanisms within the TIME (**Figure 7**).

The current study established *DDR1* as a central regulator of breast cancer progression and immune regulation by integrating multi-omics analyses with functional experimental validation, highlighting the clinical potential as a therapeutic target and prognostic biomarker. *DDR1*-targeted therapeutic strategies may improve treatment efficacy and provide a theoretical foundation for precision immunotherapy, especially in patients at high risk of recurrence.

This study elucidated a synergistic epigenetic regulatory network where DNMT3A (DNA methylation) and METTL7A (m6A modification) co-upregulate *DDR1*, activating the *DDR1/STAT3/CXCL5* axis to promote Treg infiltration, immunosuppression, and tumor recurrence. DNMT3A-mediated promoter methylation enhances *DDR1* transcription, while METTL7A stabilizes *DDR1* mRNA *via* m6A modification, forming a "DNA-RNA dual modification" mechanism. Activated *DDR1* recruits STAT3 to upregulate CXCL5, directing Treg recruitment *via* CXCR2 signaling, which suppresses anti-tumor immunity and fosters an immunosilent niche for cancer progression. Combined DNMT3A/METTL7A overexpression synergistically potentiates tumor proliferation, migration, and recurrence *in vivo*, while *DDR1* silencing disrupts this axis, reversing immunosuppression and tumor growth. The DNMT3A-METTL7A-DDR1 signature holds promise as a biomarker for recurrence prediction and therapeutic targeting, offering a novel framework for precision immunotherapy in breast cancer.

Grant support

This study was supported by the National Natural Science Foundation of China (Grant No. 82060479), Key Research and Development Program of Ningxia Hui Autonomous Region (Grant No. 2021BEG03062), and Ningxia Natural Science Fund Key Project (Grant No. 2024AAC02080).

Conflict of interest statement

No potential conflicts of interest are disclosed.

Author contributions

Conceived and designed the analysis: Zhengyang Bai, Dan Yang, Jiayi Li.
Collected the data and performed experiments: Zhengyang Bai, Dan Yang, Jiayi Li.
Contributed data or analysis tools (bioinformatics analyses) and assisted with *in vitro* and *in vivo* assays: Yaobang Liu, Bin Lian.
Supervised the study and provided clinical resources: Jinping Li.
Interpreted the data and wrote the paper: All authors.
Critically revised the manuscript and approved the final version: All authors.

Data availability statement

All data generated or analyzed during this study are included in this article and/or its supplementary material files. Further enquiries can be directed to the corresponding author.

References

1. Sung H, Ferlay J, Siegel RL, Laversanne M, Soerjomataram I, Jemal A, et al. Global cancer statistics 2020: GLOBOCAN estimates of

incidence and mortality worldwide for 36 cancers in 185 countries. CA Cancer J Clin. 2021; 71: 209-49.
2. Ibrahim M, Fathalla Z, Fatease AA, Alamri AH, Abdelkader H. Breast cancer epidemiology, diagnostic barriers, and contemporary trends in breast nanotheranostics and mechanisms of targeting. Expert Opin Drug Deliv. 2024; 21: 1735-54.
3. Binnewies M, Pollack JL, Rudolph J, Dash S, Abushawish M, Lee T, et al. Targeting TREM2 on tumor-associated macrophages enhances immunotherapy. Cell Rep. 2021; 37: 109844.
4. Moura T, Laranjeira P, Caramelo O, Gil AM, Paiva A. Breast cancer and tumor microenvironment: the crucial role of immune cells. Curr Oncol. 2025; 32: 143.
5. Plitas G, Konopacki C, Wu K, Bos PD, Morrow M, Putintseva EV, et al. Regulatory T cells exhibit distinct features in human breast cancer. Immunity. 2016; 45: 1122-34.
6. Emens LA. Breast cancer immunotherapy: facts and hopes. Clin Cancer Res. 2018; 24: 511-20.
7. Rodríguez-Bejarano OH, Parra-López C, Patarroyo MA. A review concerning the breast cancer-related tumour microenvironment. Crit Rev Oncol Hematol. 2024; 199: 104389.
8. Wen Y, Xia Y, Yang X, Li H, Gao Q. CCR8: a promising therapeutic target against tumor-infiltrating regulatory T cells. Trends Immunol. 2025; 46: 153-65.
9. Tay C, Tanaka A, Sakaguchi S. Tumor-infiltrating regulatory T cells as targets of cancer immunotherapy. Cancer Cell. 2023; 41: 450-65.
10. Lu Y, Chan YT, Tan HY, Li S, Wang N, Feng Y. Epigenetic regulation in human cancer: the potential role of epi-drug in cancer therapy. Mol Cancer. 2020; 19: 79.
11. Chen QW, Zhu XY, Li YY, Meng ZQ. Epigenetic regulation and cancer. Oncol Rep. 2013; 31: 523-32.
12. Xie Z, Zhou Z, Yang S, Zhang S, Shao B. Epigenetic regulation and therapeutic targets in the tumor microenvironment. Mol Biomed. 2023; 4: 17.
13. Baird AM, O'Byrne KJ, Gray SG. Epigenetic regulation of chemokine/chemokine receptor expression. Methods Mol Biol. 2013; 1013: 185-201.
14. Letourneur D, Danlos FX, Marabelle A. Chemokine biology on immune checkpoint-targeted therapies. Eur J Cancer. 2020; 137: 260-71.
15. Yang H, Li Y, Huang L, Fang M, Xu S. The epigenetic regulation of RNA N6-methyladenosine methylation in glycolipid metabolism. Biomolecules. 2023; 13: 273.
16. Zhang M, Zhai Y, An X, Li Q, Zhang D, Zhou Y, et al. DNA methylation regulates RNA m^6A modification through transcription factor SP1 during the development of porcine somatic cell nuclear transfer embryos. Cell Prolif. 2023; 57: e13581.
17. Jiang X, Liu B, Nie Z, Duan L, Xiong Q, Jin Z, et al. The role of m^6A modification in the biological functions and diseases. Signal Transduct Target Ther. 2021; 6: 74.
18. Sirvent A, Espie K, Papadopoulou E, Naim D, Roche S. New functions of DDR1 collagen receptor in tumor dormancy, immune exclusion and therapeutic resistance. Front Oncol. 2022; 12: 956926.
19. Wasinski B, Sohail A, Bonfil RD, Kim S, Saliganan A, Polin L, et al. Discoidin domain receptors, DDR1b and DDR2, promote tumour growth within collagen but DDR1b suppresses experimental lung metastasis in HT1080 xenografts. Sci Rep. 2020; 10: 2309.
20. Belfiore A, Malaguarnera R, Nicolosi ML, Lappano R, Ragusa M, Morrione A, et al. A novel functional crosstalk between DDR1 and the IGF axis and its relevance for breast cancer. Cell Adh Migr. 2018; 12: 305-14.
21. Deng J, Jiang R, Meng E, Wu H. CXCL5: a coachman to drive cancer progression. Front Oncol. 2022; 12: 944494.
22. Zhou SL, Dai Z, Zhou ZJ, Chen Q, Wang Z, Xiao YS, et al. CXCL5 contributes to tumor metastasis and recurrence of intrahepatic cholangiocarcinoma by recruiting infiltrative intratumoral neutrophils. Carcinogenesis. 2013; 35: 597-605.
23. Lei Q, Zhen S, Zhang L, Zhao Q, Yang L, Zhang Y. A2AR-mediated CXCL5 upregulation on macrophages promotes NSCLC progression via NETosis. Cancer Immunol Immunother. 2024; 73: 108.
24. Deng J, Kang Y, Cheng CC, Li X, Dai B, Katz MH, et al. DDR1-induced neutrophil extracellular traps drive pancreatic cancer metastasis. JCI Insight. 2021; 6: e146133.
25. Li W, Ballard J, Zhao Y, Long Q. Knowledge-guided learning methods for integrative analysis of multi-omics data. Comput Struct Biotechnol J. 2024; 23: 1945-50.
26. Bayjanov JR, Doornbos C, Ozisik O, Shin W, Queralt-Rosinach N, Wijnbergen D, et al. Integrative analysis of multi-omics data reveals importance of collagen and the PI3K AKT signalling pathway in CAKUT. Sci Rep. 2024; 14: 20731.
27. Subramanian I, Verma S, Kumar S, Jere A, Anamika K. Multi-omics data integration, interpretation, and its application. Bioinform Biol Insights. 2020; 14: 117793221989905.
28. Picard M, Scott-Boyer MP, Bodein A, Périn O, Droit A. Integration strategies of multi-omics data for machine learning analysis. Comput Struct Biotechnol J. 2021; 19: 3735-46.
29. Saeys Y, Inza I, Larrañaga P. A review of feature selection techniques in bioinformatics. Bioinformatics. 2007; 23: 2507-17.
30. Sarker IH. Machine learning: algorithms, real-world applications and research directions. SN Comput Sci. 2021; 2: 160.
31. Chen K, Shen S, Chen Y, Jiang M, Hu K, Zou Y, et al. A proteomic and RNA-seq transcriptomic dataset of capsaicin-aggravated mouse chronic colitis model. Sci Data. 2022; 9: 549.
32. Li H, Li J, Bai Z, Yan S, Li J. Collagen-induced DDR1 upregulates CXCL5 to promote neutrophil extracellular traps formation and Treg infiltration in breast cancer. Int Immunopharmacol. 2023; 120: 110235.
33. Ma P, Luo Z, Wang Q, Chen Y, Liu F, Ren C, et al. Combined activation of artificial and natural ion channels for disrupting mitochondrial ion homeostasis towards effective postoperative tumor recurrence and metastasis suppression. Theranostics. 2024; 14: 3282-99.
34. Chen YT, Shen JY, Chen DP, Wu CF, Guo R, Zhang PP, et al. Identification of cross-talk between m^6A and 5mC regulators associated with onco-immunogenic features and prognosis across 33 cancer types. J Hematol Oncol. 2020; 13: 22.
35. Tian Y, Xiao H, Yang Y, Zhang P, Yuan J, Zhang W, et al. Crosstalk between 5-methylcytosine and N^6-methyladenosine

machinery defines disease progression, therapeutic response and pharmacogenomic landscape in hepatocellular carcinoma. Mol Cancer. 2023; 22: 5.
36. Borza CM, Bolas G, Bock F, Zhang X, Akabogu FC, Zhang MZ, et al. DDR1 contributes to kidney inflammation and fibrosis by promoting the phosphorylation of BCR and STAT3. JCI Insight. 2022; 7: e150887.
37. Xue Y, Chen Y, Sun S, Tong X, Chen Y, Tang S, et al. TET2–STAT3–CXCL5 nexus promotes neutrophil lipid transfer to fuel lung adeno-to-squamous transition. J Exp Med. 2024; 221: e20240111.
38. Gao HF, Cheng CS, Tang J, Li Y, Chen H, Meng ZQ, et al. CXCL9 chemokine promotes the progression of human pancreatic adenocarcinoma through STAT3-dependent cytotoxic T lymphocyte suppression. Aging. 2020; 12: 502-17.
39. Yin H, Ju Z, Zheng M, Zhang X, Zuo W, Wang Y, et al. Loss of the m^{6}A methyltransferase METTL3 in monocyte-derived macrophages ameliorates Alzheimer's disease pathology in mice. PLoS Biol. 2023; 21: e3002017.
40. Qaria MA, Xu C, Hu R, Alsubki RA, Ali MY, Sivasamy S, et al. Ectoine globally hypomethylates DNA in skin cells and suppresses cancer proliferation. Mar Drugs. 2023; 21: 621.
41. Quarto G, Li Greci A, Bizet M, Penning A, Primac I, Murisier F, et al. Fine-tuning of gene expression through the Mettl3-Mettl14-Dnmt1 axis controls ESC differentiation. Cell. 2025; 188: 998-1018.e26.
42. Lu W, Yang S. METTL3/IGF2BP1 promotes the development of triple-negative breast cancer by mediating m6A methylation modification of PRMT7. Tissue Cell. 2025; 93: 102690.
43. Cheng M, Sheng L, Gao Q, Xiong Q, Zhang H, Wu M, et al. The m^{6}A methyltransferase METTL3 promotes bladder cancer progression via AFF4/NF-κB/MYC signaling network. Oncogene. 2019; 38: 3667-80.
44. Wang J, Wang L, Qiang W, Ge W. The role of DDR1 in cancer and the progress of its selective inhibitors. Bioorg Chem. 2025; 154: 108018.
45. Wu M, Ma W, Lv G, Wang X, Li C, Chen X, et al. DDR1 is identified as an immunotherapy target for microsatellite stable colon cancer by CRISPR screening. npj Precis Onc. 2024; 8: 253.
46. Schott AF, Goldstein LJ, Cristofanilli M, Ruffini PA, McCanna S, Reuben JM, et al. Phase Ib Pilot study to evaluate reparixin in combination with weekly paclitaxel in patients with HER-2–negative metastatic breast cancer. Clin Cancer Res. 2017; 23: 5358-65.
47. Lian B, Yan S, Li J, Bai Z, Li J. HNRNPC promotes collagen fiber alignment and immune evasion in breast cancer via activation of the VIRMA-mediated TFAP2A/DDR1 axis. Mol Med. 2023; 29: 103.
48. Lu A, Wang W, Wang-Renault SF, Ring BZ, Tanaka Y, Weng J, et al. 5-Aza-2′-deoxycytidine advances the epithelial–mesenchymal transition of breast cancer cells by demethylating Sipa1 promoter-proximal elements. J Cell Sci. 2020; 133: jcs236125.
49. Shuai Y, Ma Z, Ju J, Li C, Bai X, Yue J, et al. The N6-methyladenosine writer METTL3 promotes breast cancer progression through YTHDF2-dependent posttranscriptional silencing of GSDMD. Apoptosis. 2024; 30: 226-38.
50. Cesaro B, Iaiza A, Piscopo F, Tarullo M, Cesari E, Rotili D, et al. Enhancing sensitivity of triple-negative breast cancer to DNA-damaging therapy through chemical inhibition of the m6A methyltransferase METTL3. Cancer Commun (Lond). 2023; 44: 282-6.
51. Lu QP, Chen WD, Peng JR, Xu YD, Cai Q, Feng GK, et al. Antitumor activity of 7RH, a discoidin domain receptor 1 inhibitor, alone or in combination with dasatinib exhibits antitumor effects in nasopharyngeal carcinoma cells. Oncol Lett. 2016; 12: 3598-608.
52. Zhang X, Hu Y, Pan Y, Xiong Y, Zhang Y, Han M, et al. DDR1 promotes hepatocellular carcinoma metastasis through recruiting PSD4 to ARF6. Oncogene. 2022; 41: 1821-34.
53. Sohrabei S, Moghaddasi H, Hosseini A, Ehsanzadeh SJ. Investigating the effects of artificial intelligence on the personalization of breast cancer management: a systematic study. BMC Cancer. 2024; 24: 852.
54. Zhu F, Xu D. Predicting gene signature in breast cancer patients with multiple machine learning models. Discov Oncol. 2024; 15: 516.
55. Sharma A, Debik J, Naume B, Ohnstad HO; Oslo Breast Cancer Consortium (OSBREAC); Bathen TF, et al. Comprehensive multi-omics analysis of breast cancer reveals distinct long-term prognostic subtypes. Oncogenesis. 2024; 13: 22.
56. Rashid MM, Selvarajoo K. Advancing drug-response prediction using multi-modal and -omics machine learning integration (MOMLIN): a case study on breast cancer clinical data. Brief Bioinform. 2024; 25: bbae300.
57. Yang J, Xu J, Wang W, Zhang B, Yu X, Shi S. Epigenetic regulation in the tumor microenvironment: molecular mechanisms and therapeutic targets. Signal Transduct Target Ther. 2023; 8: 210.
58. Huang W, Zhu Q, Shi Z, Tu Y, Li Q, Zheng W, et al. Dual inhibitors of DNMT and HDAC induce viral mimicry to induce antitumour immunity in breast cancer. Cell Death Discov. 2024; 10: 143.
59. Li CJ, Tzeng YDT, Chiu YH, Lin HY, Hou MF, Chu PY. Pathogenesis and potential therapeutic targets for triple-negative breast cancer. Cancers (Basel). 2021; 13: 2978.
60. Zhong X, Zhang W, Sun T. DDR1 promotes breast tumor growth by suppressing antitumor immunity. Oncol Rep. 2019; 42: 2844-2854.
61. Baltes F, Caspers J, Henze S, Schlesinger M, Bendas G. Targeting discoidin domain receptor 1 (DDR1) signaling and its crosstalk with β1-integrin emerges as a key factor for breast cancer chemosensitization upon collagen type 1 binding. Int J Mol Sci. 2020; 21: 4956.
62. Brunetti L, Gundry MC, Goodell MA. DNMT3A in leukemia. Cold Spring Harb Perspect Med. 2016; 7: a030320.
63. Man X, Li Q, Wang B, Zhang H, Zhang S, Li Z. DNMT3A and DNMT3B in breast tumorigenesis and potential therapy. Front Cell Dev Biol. 2022; 10: 916725.
64. Disteldorf EM, Krebs CF, Paust HJ, Turner JE, Nouailles G, Tittel A, et al. CXCL5 drives neutrophil recruitment in TH17-mediated GN. J Am Soc Nephrol. 2015; 26: 55-66.
65. Rich BE, Leder P. Transgenic expression of interleukin 7 restores T cell populations in nude mice. J Exp Med. 1995; 181: 1223-8.

66. Dosch HM, White D, Grant C. Reconstitution of nude mouse T cell function in vivo: IL 2-independent effect of human T cells. J Immunol. 1985; 134: 336-42.
67. Kim ME, Kim DH, Lee JS. FoxO transcription factors: applicability as a novel immune cell regulators and therapeutic targets in oxidative stress-related diseases. Int J Mol Sci. 2022; 23: 11877.
68. Lee BC, Lee J. Cellular and molecular players in adipose tissue inflammation in the development of obesity-induced insulin resistance. Biochim Biophys Acta. 2014; 1842: 446-62.
69. Sun X, Wu B, Chiang HC, Deng H, Zhang X, Xiong W, et al. Tumour DDR1 promotes collagen fibre alignment to instigate immune exclusion. Nature. 2021; 599: 673-8.

Cite this article as: Bai Z, Yang D, Li J, Liu Y, Lian B, Li J. Coordinated DNA methyltransferase 3A and methyltransferase-like 7A activity reprograms the tumor microenvironment through discoidin domain receptor 1 signaling. Cancer Biol Med. 2026; 23: 107-132. doi: 10.20892/j.issn.2095-3941.2025.0261